remote sensing

MDPI

Review

Application of LiDAR Sensors for Crop and Working Environment Recognition in Agriculture: A Review

Md Rejaul Karim [1], Md Nasim Reza [1,2], Hongbin Jin [2], Md Asrakul Haque [1], Kyu-Ho Lee [1,2], Joonjea Sung [3] and Sun-Ok Chung [1,2,*]

[1] Department of Agricultural Machinery Engineering, Graduate School, Chungnam National University, Daejeon 34134, Republic of Korea; mrkarim@o.cnu.ac.kr (M.R.K.); reza5575@cnu.ac.kr (M.N.R.); asrak.bzs13@o.cnu.ac.kr (M.A.H.); elkyu0927@cnu.ac.kr (K.-H.L.)
[2] Department of Smart Agricultural Systems, Graduate School, Chungnam National University, Daejeon 34134, Republic of Korea; jhb0117@o.cnu.ac.kr
[3] FYD Co., Ltd., Suwon 16676, Republic of Korea; enature1004@fydkr.com
* Correspondence: sochung@cnu.ac.kr; Tel.: +82-42-821-6712

Abstract: LiDAR sensors have great potential for enabling crop recognition (e.g., plant height, canopy area, plant spacing, and intra-row spacing measurements) and the recognition of agricultural working environments (e.g., field boundaries, ridges, and obstacles) using agricultural field machinery. The objective of this study was to review the use of LiDAR sensors in the agricultural field for the recognition of crops and agricultural working environments. This study also highlights LiDAR sensor testing procedures, focusing on critical parameters, industry standards, and accuracy benchmarks; it evaluates the specifications of various commercially available LiDAR sensors with applications for plant feature characterization and highlights the importance of mounting LiDAR technology on agricultural machinery for effective recognition of crops and working environments. Different studies have shown promising results of crop feature characterization using an airborne LiDAR, such as coefficient of determination (R^2) and root-mean-square error (RMSE) values of 0.97 and 0.05 m for wheat, 0.88 and 5.2 cm for sugar beet, and 0.50 and 12 cm for potato plant height estimation, respectively. A relative error of 11.83% was observed between sensor and manual measurements, with the highest distribution correlation at 0.675 and an average relative error of 5.14% during soybean canopy estimation using LiDAR. An object detection accuracy of 100% was found for plant identification using three LiDAR scanning methods: center of the cluster, lowest point, and stem–ground intersection. LiDAR was also shown to effectively detect ridges, field boundaries, and obstacles, which is necessary for precision agriculture and autonomous agricultural machinery navigation. Future directions for LiDAR applications in agriculture emphasize the need for continuous advancements in sensor technology, along with the integration of complementary systems and algorithms, such as machine learning, to improve performance and accuracy in agricultural field applications. A strategic framework for implementing LiDAR technology in agriculture includes recommendations for precise testing, solutions for current limitations, and guidance on integrating LiDAR with other technologies to enhance digital agriculture.

Keywords: digital agriculture; LiDAR sensor; agricultural field machinery; crop recognition; agricultural working environment

Citation: Karim, M.R.; Reza, M.N.; Jin, H.; Haque, M.A.; Lee, K.-H.; Sung, J.; Chung, S.-O. Application of LiDAR Sensors for Crop and Working Environment Recognition in Agriculture: A Review. *Remote Sens.* **2024**, *16*, 4623. https://doi.org/10.3390/rs16244623

Academic Editors: Qinghua Xie, Yaqian He and Fang Fang

Received: 23 October 2024
Revised: 25 November 2024
Accepted: 1 December 2024
Published: 10 December 2024

1. Introduction

Agriculture is one of the most important sectors of the global economy, providing food, raw materials, and employment to millions of people worldwide [1]. As the global population continues to grow, the demand for agricultural products has increased, necessitating advancements in technology to increase productivity, enhance sustainability, and ensure food security [2–4]. Among the many technologies being explored, Light Detection and

Ranging (LiDAR) has emerged as a promising tool for various applications in agriculture, particularly in crop and working environment recognition [5]. The precision, accuracy, and versatility of LiDAR make it a valuable resource for enhancing decision-making processes, optimizing resource management, and enabling automation in agricultural practices [5,6].

LiDAR technology, originally developed for geological and military applications, has gained substantial attention in the agricultural sector in recent years [7–10]. LiDAR is a remote sensing technology that works by emitting laser pulses and measuring the time taken for those pulses to reflect back after hitting objects [11–14]. The time-of-flight (ToF) data are used to generate highly accurate three-dimensional (3D) maps of the environment by periodically emitting pulses of light, detecting the resulting collisions, and building a detailed map of the environment for enabling a wide range of agricultural applications [15,16]. A LiDAR sensor typically uses multiple laser pulses, which directly impacts the performance of the sensor in terms of data resolution, accuracy, and scanning efficiency. Key factors such as operational range, error estimation, and scanning frequency also play critical roles in determining the effectiveness of the sensor, where higher pulse rates improve the detail and density of the point cloud data but may also increase computational demands and sensitivity to noise or interference, particularly in dense or complex environments [14,17]. LiDAR is an active sensor with a laser that emits light pulses, which can be used alongside Global Positioning System (GPS) receivers to provide precise geospatial location data, with the reflected light data processed and stored as spatial coordinates to form a point cloud representing the 3D structure of the scanned environment [5,16]. The precision, range, and detailed point cloud data make LiDAR invaluable in agriculture, forestry, and autonomous systems, especially in challenging environments such as low-light conditions [5]. The ability to capture detailed surface structures enables high-resolution maps and models, supporting precision, efficiency, and automation in modern agricultural technology [5,12]. LiDAR sensors are independent of ambient light, generating their own laser pulses, allowing for effective use both day and night, as well as in various weather conditions, such as cloud cover or shade [18]. In contrast, sensors such as RGB (red, green, blue) and multispectral cameras rely on sunlight and are susceptible to lighting variations, which can lead to errors in plant feature measurements. Moreover, LiDAR sensors provide millimeter–centimeter-level accuracy, making them ideal for measuring small variations in plant height and canopy density [6,19]. This precision surpasses that of ultrasonic sensors and RGB cameras, which are less effective for structural measurements. For predicting crop yields and monitoring plant size, this accuracy is essential. LiDAR can also penetrate dense canopies, capturing both upper and lower plant structures, which multispectral or RGB cameras may miss [20]. This capability allows for detailed analysis of canopy structure, leaf area index (LAI), and growth, offering valuable insights into plant health and growth dynamics. These data can be used to develop predictive models for yield estimation, nutrient requirements, and pest management strategies.

Technological advancements in agriculture over the past decade have been driven by the need for precision farming to optimize inputs and minimize environmental impact [21,22]. As sustainable farming practices and climate change awareness grow, smart farming technologies, including LiDAR, are increasingly being adopted. In agriculture, the application of LiDAR sensors in crop and working environment recognition goes beyond mere mapping. In crop management, LiDAR is being used to assess plant structural features such as height, spacing, row distances, canopy volume, and canopy structure analysis, as well as to estimate biomass and even detect diseases [5,6,23–30]. In tree crops and vineyards, LiDAR data can be employed to analyze canopy structure, which directly impacts sunlight distribution, water usage, and overall plant health [31–33]. Additionally, the high-resolution 3D data captured by LiDAR sensors are increasingly being integrated into machine learning algorithms, enabling autonomous vehicles and drones to navigate complex agricultural environments with minimal human intervention [34,35]. This enhances not only the efficiency but also the safety of farm operations, as it allows for accurate, real-time recognition of obstacles, terrain changes, and crop variations.

The precision offered by LiDAR is particularly beneficial for addressing the challenges of heterogeneous farm environments, where variations in soil composition, topography, and microclimate can significantly impact crops' health and yield [5,6,34]. Traditional farming methods often rely on uniform treatment of entire fields, which can lead to overuse of resources in some areas and underuse in others. By providing detailed information on field variability, LiDAR sensors enable precision farming techniques such as variable rate application, where inputs are applied based on the specific needs of different areas within a field. This leads to better resource efficiency, reduced waste, and improved crop performance.

In the working environment, LiDAR sensors are proving invaluable for autonomous machinery and robotics in agriculture. As farms move toward automation, the need for machinery to safely and efficiently navigate through fields becomes paramount. LiDAR provides the high-resolution spatial data required for autonomous systems to detect field boundaries, ridges and furrows, and topographical obstacles, as well as to map terrain and make real-time decisions about navigation paths [35–40]. This is particularly useful in large-scale farming operations, where the sheer size of fields makes manual navigation impractical and inefficient. For crop phenotyping and field scouting, LiDAR sensors are highly reliable due to their low failure rates and high accuracy [41]. Moreover, LiDAR can be used to create digital twins of farm environments, providing farmers with a virtual replica of their fields for planning and monitoring purposes [42,43]. LiDAR sensors are essential in robotics and autonomous systems for providing real-time, high-resolution spatial data. This makes these sensors ideal for farming robots and drones to navigate fields, avoid obstacles, and perform precise tasks such as weeding, harvesting, and topographical mapping [38].

Unlike ultrasonic or ToF sensors, such as radar or sonar, which offer less detail and range, LiDAR enhances the effectiveness of automation in agriculture. LiDAR can map not only plants or crops but also their surrounding environments, such as ridges, field boundaries, and soil surfaces, making it a comprehensive tool [16]; it captures land topography, helping identify features that affect planting efficiency. Unlike sensors such as hyperspectral or RGB cameras, which capture surface features, LiDAR integrates both plant and environmental data, offering an integrated view for optimizing farm management. LiDAR collects data in real-time, enabling immediate analysis of plant features during field operations, which is crucial for dynamic decision-making in precision agriculture [44]. In contrast, many other sensors, such as those relying on post-processing (e.g., photogrammetry), cannot provide the same immediacy in data availability [5,6]. LiDAR can be mounted on various platforms, from handheld devices and ground vehicles to drones and airplanes, making it scalable for different farm sizes and applications, with large coverage areas and 3D structural details [23,26,45]. One of the primary challenges faced in crop management is the accurate recognition and classification of plant species and their growth stages [46,47]. Traditionally, visual inspection and manual measurements have been the primary methods for assessing crops' health and development. However, these methods are time-consuming, labor-intensive, and prone to human error [48–50].

The integration of LiDAR data with other remote sensing technologies further enhances its potential for crop and working environment recognition. Integrating LiDAR with multispectral or hyperspectral imaging enhances this recognition [51]. While multispectral cameras can capture plant health indicators such as chlorophyll content, LiDAR provides structural data [51,52]. Integration offers a more comprehensive understanding of crop conditions, enabling early intervention and targeted treatments to address stress, disease, and nutrient deficiencies.

Despite its many advantages, the adoption of LiDAR technology in agriculture faces challenges. LiDAR's performance can be affected by several challenges, including complex plant structures, occlusion, resolution and accuracy limitations, and plant movement due to wind during data collection. Additionally, moisture, dust, or debris can scatter laser beams, introducing noise [23,26]. Uneven terrain and plant-to-plant variability further complicate distinguishing plants from their environment, making accurate feature characterization

more difficult [53]. LiDAR generates a large volume of data in agricultural applications. The high-resolution point clouds require substantial computational power and storage for processing and analysis. The high cost of sensors and the complexity of data processing are often cited as obstacles to the widespread use of LiDAR, particularly for small and medium-sized farms [5]. However, advancements in sensor technology and the growing availability of cloud-based data processing platforms are helping to reduce these barriers. Furthermore, as technology matures and becomes more accessible, it is expected that the cost of LiDAR sensors will continue to decrease, making them a viable option for a broader range of agricultural applications.

LiDAR holds significant potential for advancing smart and digital agriculture. The labor-intensive nature of traditional farming, labor shortages, and the migration of young workers to other sectors make LiDAR a viable solution. The use of LiDAR in agricultural machinery has grown in response to these challenges, showing promise in crop recognition and operational environment detection. Therefore, this review aimed to explore the application of LiDAR in agriculture, focusing on crop and agricultural working environment recognition.

2. LiDAR Sensor Classification and Applications in Agriculture

Studies in the literature highlight four LiDAR-based scanning systems: ground LiDAR scanning (GLS), stationary LiDAR scanning (SLS), airborne LiDAR scanning (ALS), and mobile LiDAR scanning (MLS) [54]. According to the scanning angle, LiDAR is mainly classified into two classes: airborne and terrestrial and LiDAR [55,56]. Based on typical operations, terrestrial LiDAR systems often perform horizontal scanning with a 360° field of view. Depending on the system, the scanning may be one-dimensional (1D), capturing distances along a single axis, or two-dimensional (2D), where horizontal scanning is combined with vertical angular movements to capture a plane of data. Airborne LiDAR scans the objects/areas downward, with a vertical scanning angle of 180°; it is typically mounted on aircraft or drones, emitting lasers toward the ground, which are reflected and returned to the LiDAR for creating accurate 3D terrain maps that are often integrated with other remote sensing technologies [57]. Airborne LiDAR is subclassified into bathymetric and topographic LiDAR. Bathymetric LiDAR is used near coastlines, shores, and banks to measure underwater elevation and water depth simultaneously [56]. Topographic LiDAR, typically deployed on airborne systems, is used for large-scale applications such as forestry, landscape assessment, urban planning, and crop monitoring [16,45,56,58–63]. Terrestrial LiDAR, on the other hand, includes mobile and static types. Mobile terrestrial LiDAR, which operates from ground vehicles or handheld platforms, shares some applications with topographic LiDAR, such as landscape and infrastructure analysis, but is primarily suited for detailed mapping of road signs, light poles, and other urban features [64,65]. Static terrestrial LiDAR is primarily used for engineering surveys and fixed-point measurements, and both types of terrestrial LiDAR are applied in agriculture for assessing landscapes, estimating leaf area, predicting crop biomass, and detecting weeds [58,66–70]. Figure 1 shows a detailed classification of LiDAR sensors, along with their various applications in agriculture.

LiDAR sensors have a wide range of uses in agriculture. They are widely used in agricultural models such as digital elevation models (DEMs), digital terrain models (DTMs), and digital surface models (DSMs) [16,71]. LiDAR is being used for crop classification, inspection of crop viability, crop mapping, cloud profiling, collision avoidance, obstacle detection in autonomous traveling, and soil resource conservation in agriculture [72–74]. LiDAR sensors are important in agriculture for crop recognition and working environment detection, which enhance input efficiency, productivity, and safety, with LiDAR-equipped tractors using 3D data for obstacle detection and object classification [55,57].

LiDAR has seen widespread utilization in agricultural field machinery [75–78], object detection [79–82], and high-throughput crop phenotyping [83–86]. Several studies have demonstrated LiDAR applications in agricultural working environments using various

platforms, such as robots [81], tractors [80], speed sprayers [87], and the AgRob V16 agricultural robotic platform [76]. Airborne platforms are used to estimate the crown structure of trees using both waveform and discrete return recordings, which are techniques used in forestry, agriculture, and environmental management [27]. Several parameters, including tree height, crown size, shape, and volume, have been measured using LiDAR; it has been used for the segmentation and reconstruction of plant parts, as well as the detection and quantification of fruits [79,80]. ALS is used for estimating plant height [88,89] and soil properties [90,91], as well as for monitoring tree health [92,93]. TLS and MLS offer higher spatial resolution, provide more detailed crop characterization [24], and are popular for various agricultural applications. Table 1 illustrates the classification of LiDAR sensors with several applications in agriculture.

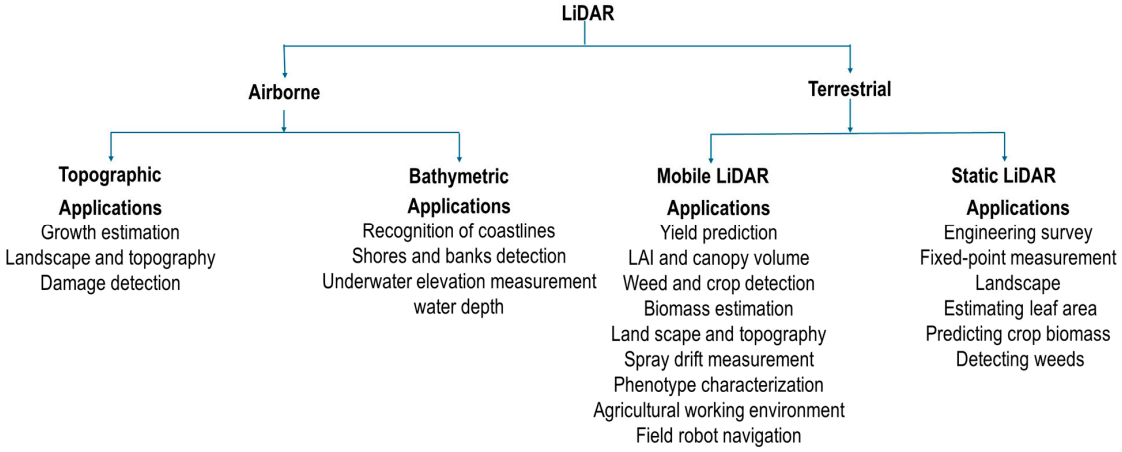

Figure 1. Schematic diagram of LiDAR sensor classification and their applications in agriculture.

Table 1. Common uses of different types of LiDAR systems in agricultural applications.

LiDAR	Application	Model	Specifications			Reference
			Operating Range (m)	Error (m)	Scanning Frequency (Hz)	
ALS	Plant health monitoring	VLP-16	100	30	20	[90]
		RIEGL VUX-1UAV	1.5–1415	5–10	1200	[91]
	Plant height monitoring	VLP-16	100	30	5–20	[87]
		LMS511-10100 PRO	40	6–14	25–100	[27]
		RIEGL VUX-1UAV	1.5–1415	5–10	1200	[93]
		HDL-32	80–100	20	5–20	[24]
	Yield estimation	VLP-16 Puck-Lite	100	30	5–20	[94]
	Tree detection	VLP-16	100	30	5–20	[95]
TLS and MLS	Dry matter	LMS400 PRO	3	3	300–500	[96]
	Plant health monitoring	FARO Focus X330	30–330	2	97	[97]
		VLP-16 Puck	100	30	5–20	[98]
		LMS111	20	12	25–50	[99]
	Canopy structure estimation	LMS400-2000	3	3	300–500	[92]
	Plant growth	LMS511 PRO SR	80	6–14	25–100	[100]
	Volume estimation	UTM-30LX-EW	30	30–50	40	[101]
	Yield estimation	LMS400 PRO	3	3	300–500	[102]
	Tree structure digitization	RIEGL VZ-400 V	5–1000	10–15	30–300	[103]
		LMS111	20	12	25–50	[104]
		UTM-30LX	30	30–50	40	[105]

3. Crop Feature Recognition

Accurate crop characterization and recognition of plant features are essential for monitoring plant growth and implementing precise management practices in crop production [106]. LiDAR technology captures detailed information about plant structure, including height, canopy area and volume, and crop spacing, allowing for precise identification and monitoring of crop health issues such as diseases or nutrient deficiencies and enabling farmers to make decisions about irrigation management [107]. Crop characterization is a key process in precision agriculture but remains challenging due to the unstructured field environment and the diversity of crops and plants. Despite these challenges, LiDAR technology has become widely used in agriculture, particularly for crop recognition applications.

3.1. Plant Height Measurement

Plant height significantly impacts agricultural outcomes, particularly grain yield traits. Traditional methods relied on indirect methods such as geometric formulae and handheld laser rangefinders, as shown in Figure 2, which are time-intensive and costly. LiDAR-estimated data, compared to conventional measured data using Equation (1), proved efficient and reliable for plant height measurement [66,108–111].

$$H = A + B = D(\tan\theta + \tan\varnothing) \quad (1)$$

where H is the estimated total height of the tree (m), D is the distance from the viewpoint to base (m), B is the height of the crown from the base (m), Φ is the angle to the top of the tree (°), θ is the angle to the bottom of the tree (°), and A is the length of the crown (m).

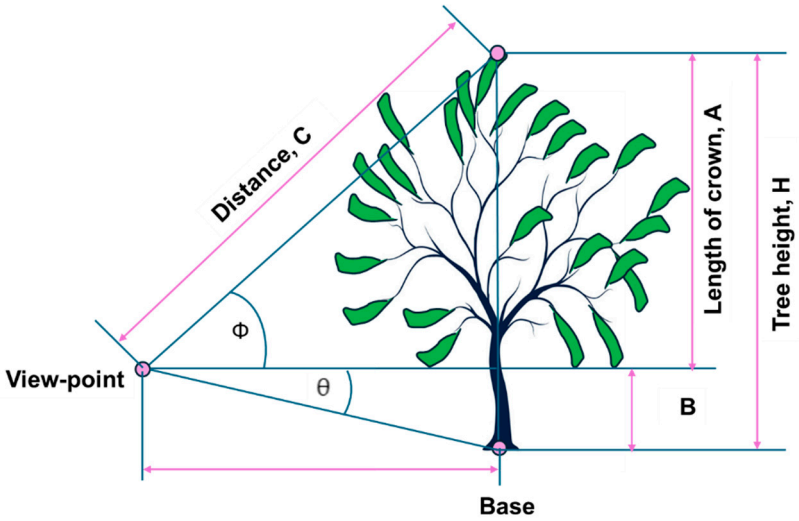

Figure 2. Conventional tree height measurement in the field using trigonometric principles.

LiDAR is widely used in precision agriculture for 3D plant structure measurement. Testing LiDAR in wheat fields showed strong correlations with canopy height, achieving an R^2 of 0.99 and RMSE of 0.017 m [108,112]. Density-based spatial clustering of applications with noise (DBSCAN), a data clustering algorithm, the sample consensus initial alignment (SCA_IA) algorithm to sample a large number of candidate correspondences, the iterative closest point (ICP) algorithm, and a point cloud library were used for efficient LiDAR data processing [113]. LiDAR can deliver data more efficiently than other sensors for crop phenotype characterization [114]. Another study assessed plant height, plant crown diameter, and panicle height and diameter. The R^2 values for these features were 0.83, 0.94, 0.90, and 0.90, respectively, with root-mean-square errors (RMSEs) of 6.8 cm, 1.82 cm, 5.7 mm, and 7.8 mm, respectively. The findings demonstrated a strong correlation between the point cloud data and manually collected measurements for plant feature characterization,

suggesting that the 3D LiDAR system enabled the quick and accurate measurement of sorghum plants' features [115].

High spatial resolution, minimal beam divergence, and adaptability to ambient light conditions have made LiDAR a widely accepted sensor for 3D plant structure reconstruction [59,65,66]; it can efficiently construct geometric maps of vegetation and canopy structures, providing realistic aboveground plant models using technologies such as time of flight (ToF). LiDAR has been used in crop analysis, where a crop surface model (CSM) was developed with a 4% elevation difference to measure crop height [62]. LiDAR has also been used in agricultural field machinery platforms for the precise estimation of plant and tree heights [116–120]. Statistical models are used to combine LiDAR scanning frequencies of crop density and spike number, while CSMs and DTMs are used to determine plant height by subtracting the values [58]. Airborne LiDAR can process data to create cornfield height maps and effectively measure plant height by assessing differences in image points [64]. For rice plants, LiDAR acquired 3D point cloud data, determining height as the difference between the top and bottom positions [63,121,122]. In wheat fields, LiDAR demonstrated strong correlations with canopy height, achieving an R^2 of 0.99 and an RMSE of 0.017 m [108,112].

A 2D LiDAR mounted on a high-clearance tractor measured cotton plant height with 98% accuracy and an RMSE of 65 mm, using a 0.5° angular resolution during the tree scanning [123]. LiDAR was also integrated with the "Phenomobile" platform for wheat height estimation and compared with RGB and normalized difference vegetation index (NDVI) data [108]. LiDAR was used to measure plant height and canopy density with a single scan [124]. In field conditions, LiDAR mounted on a tractor provided satisfactory height measurement results for wheat (R^2 = 0.78, RMSE = 3.4 cm), sugar beet (R^2 = 0.70, RMSE = 7.4 cm), potato (R^2 = 0.50, RMSE = 12 cm), and cotton (R^2 = 0.98) [39,108,125–127]. LiDAR was also tested for the precise measurement of canopy structure and height [128]. A least-squares surface fitting algorithm estimated the average crop height of giant miscanthus with an average error of 5.08% [119]. Additionally, LiDAR was tested to estimate the ground surface, and a 3D model for assessing sweet potato growth characteristics was constructed [120]. A Velodyne HDL64-S3 LiDAR mounted on a mobile robot and using a robotic operating system (ROS) estimated maize plants' height through point cloud analysis [113], involving point cloud registration, merging, and single-plant height computation [115,129], as shown in Figure 3.

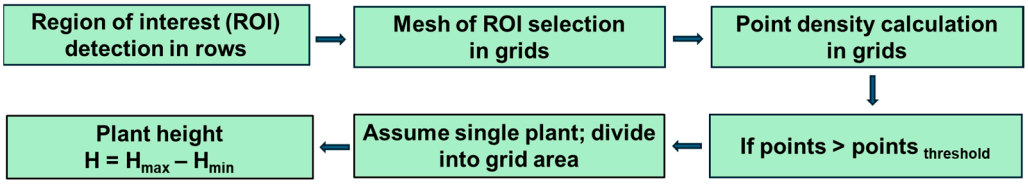

Figure 3. Plant height estimation flowchart using a LiDAR sensor mounted on the autonomous platform.

Airborne LiDAR was tested for measuring wheat, sugar beet, potato, and cotton plants' height, achieving good results. For wheat plant height estimation, LiDAR provided results with a root-mean-square error (RMSE) of 0.05 m and an R^2 of 0.97 [101]. Another study showed field validation results with r^2 of 0.99 and root-mean-square error of 0.017 m for LiDAR measurements in a wheat field [113]. The point cloud-estimated height of sugar beet plants was compared with measured height in another study, where good correlations were found between estimated and measured plant height, with R^2 = 0.88 and RMSE = 5.2 cm [129]. The biomass of several crops was estimated by using the 3-dimensional profile index (3DPI) algorithm [127], where crop height was determined by averaging the heights of the highest points within each square meter. The LiDAR 3D point cloud was segmented into layers, and the fraction of points within each layer was calculated with respect to the total number of points. The fractions were then summed,

and the resulting 3DPI values were correlated with biomass using a linear function. The 3DPI algorithm performed well in estimating biomass for sugar beet, with R^2 = 0.68 and RMSE = 17.47 gm^{-2} [127], while for winter wheat the values were R^2 = 0.82 and RMSE = 13.94 gm^{-2} [127]. Similarly, the height estimates were accurate for sugar beet, with R^2 = 0.70 and RMSE = 7.4 cm, and for wheat, with R^2 = 0.78 and RMSE = 3.4 cm. However, for potatoes, the plant height estimates were less reliable (R^2 = 0.50 and RMSE = 12 cm), likely due to the complex canopy structure and the ridged terrain where the potatoes were grown [127]. In a lab test, individual cotton plants were scanned with LiDAR at an angular resolution of 0.5°, yielding an R^2 value of 1.00 and an RMSE of 3.46 mm when compared to manual measurements. In field tests using the same angular resolution, the combined LiDAR–HTP system achieved an average R^2 value of 0.98 and an RMSE of 65 mm for estimating the cotton plant's height, also in comparison to manual measurements [53].

3.2. Canopy Area and Volume Measurements

Tree canopy measurement can characterize the tree structure [130–134] and is essential for determining growth and photosynthesis [135]. For tree canopy measurement, terrestrial LiDAR achieved an R^2 of 0.77 for canopy volume–yield correlation [136], and a mobile 3D LiDAR reported correlations of 0.81 and 0.51 for manual and automatic measurements of apple trees and grapevines [137], respectively. The voxel grid method proved more accurate than the convex hull method for canopy measurement [87,98]. Additionally, an alpha shape technique applied to a generated 3D tree shape was more effective than the convex method, avoiding overestimation [138]. Several voxel grid approaches, such as convex hull, segmented convex hull, cylinder-based modeling techniques, and a 3D occupancy grid approach, were used for apple tree canopy measurement. Among these approaches, the segmented convex hull method showed 42% greater accuracy than the convex hull method, and the 3D occupancy grid approach closely matched the actual template volume during canopy measurement [138,139].

A LiDAR sensor on a tractor, alongside a monocular vision system, was used to estimate plum tree canopy cover [140]. Voxel grid approaches were applied for tree canopy area measurement [141]. LiDAR sensors have been widely used for sensor-based research in tree canopy area measurement [88,98]. A 2D terrestrial LiDAR was tested for estimating key structural and geometric characteristics of plant canopies [142]. LiDAR has emerged as a preferred system for canopy volume calculations due to its accuracy, speed, and versatility [143]. A LiDAR sensor using the ToF principle effectively measured the canopy area [100]. A LiDAR mounted on a tractor was used in vineyards and apple orchards for distance measurement, with commercial software handling the data acquisition and processing [101]. The tractor operated at speeds of 1–2 kmh^{-1}, and the sensor demonstrated accuracy within ±15 mm, with a standard deviation of 5 mm, at distances up to 8 m and angular resolutions of 1°, 0.5°, and 0.25°. Another study measured the canopy volume of apple and pear orchards using both LiDAR and manual methods, showing a strong correlation [144]. Additionally, LiDAR was used to measure soybean canopy, where the mean shift algorithm was employed to extract individual plants [145]. The study reported a relative error of 11.83% between sensor and manual measurements, with a highest distribution correlation of 0.675 and an average relative error of 5.14%.

Airborne LiDAR, known for its efficiency and cost-effectiveness in large-scale data acquisition, utilized the canopy height model (CHM) to measure canopy height and distinguish individual trees [145]. A CHM was produced by interpolating first-return LiDAR data normalized by a DTM. LiDAR has proven to be the most accurate method for assessing canopy features, offering reliable canopy area estimations in numerous studies. However, CHMs have limitations, such as difficulties with crown shape and tree overlaps, which complicate frequent height estimation and lead to surface errors [145].

3.3. Crop Spacing Measurement

LiDAR sensors are highly regarded for ground-based research, particularly for locating and classifying plants [145]. Widely used in various agricultural applications, these sensors have been used for tasks such as 3D tree representation for precise pesticide applications [145,146] and plant location in the field [147]. LiDAR has been tested in field conditions, projecting cloud points within the region of interest (ROI) and measuring row spacing by clustering 3D point cloud data [113]. Data processing algorithms, including scan registration and stalk recognition, were applied to enhance the LiDAR data, reducing misidentification errors and achieving a 5.5% plant counting error with an RMSE of 1.9 cm. Spacing measurements were compared to manual ground-truth data for validation [113,147].

These sensors provide rapid distance measurements along a line at high scanning rates [148]. The distance to target objects can be determined based on laser beam transmission and reception times, as shown in Figure 4. Three types of optical sensors, including LiDAR and an RGB camera, were tested for plant distance measurement, achieving an accuracy of 90% at distances of 880 nm and 905 nm [53]. Three LiDAR scanning methods—center of the cluster, lowest point, and stem–ground intersection—were used for plant detection, achieving 100% object detection accuracy and 3–21% plant detection accuracy [103]. Table 2 provides a summary of various studies and applications of these sensors in crop recognition.

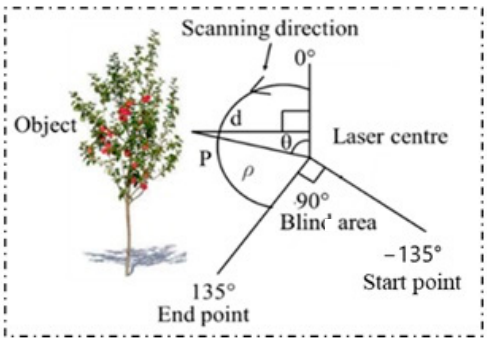

Figure 4. LiDAR sensor detection range diagram for distance measurement of target.

Table 2. Summary of crop recognition applications using different LiDAR sensors.

Parameters	Crops	Methods/Algorithms	Conditions	References
Plant height	Rice, cotton, wheat, sugar beet, potato, sweet potato, maize	Shortest-distance measurement (SDM), 3D reconstruction, least-squares (LS) surface fitting, CHM, 3D PCD map	Field/ laboratory	[66,89,108–112,114,116,118,119,136,147]
Canopy volume	Rice, wheat, potato, maize, sugar beet, cotton	Three-dimensional (3D) plant surface reconstruction (PSR), multi-temporal method (MTM), convex hull, voxel grid, RANSAC and DBSCAN	Field	[114,135,139,142,143,145,149]
Plant/tree distance	Maize, rice, wheat, orchard trees	Shortest-distance measurement (SDM)	Field	[142,143,146–148,150,151]

4. Working Environment Feature Recognition

LiDAR is increasingly used in agriculture for working environment recognition, playing a crucial role in enhancing the efficiency and safety of field operations. By emitting laser pulses and capturing detailed 3D spatial data, LiDAR enables precise mapping of farm environments, including obstacles, terrain variations, and machinery pathways [54,57]. These data are essential for autonomous machinery such as tractors and drones, which rely on them for navigation, obstacle avoidance, and real-time decision-making. In addition to machinery navigation, LiDAR assists in identifying field boundaries, ridges, and soil surfaces, making it a valuable tool for optimizing land management and resource allocation [152,153]; it can detect uneven terrain, assess field conditions, and ensure safe machinery operation, reducing the risk of accidents and improving workflow efficiency [153,154].

4.1. Field Boundary and Ridge Detection

A 3D LiDAR was tested for ground modeling and object recognition using agricultural field machinery, utilizing a voxel grid model combined with discriminative analysis for recognizing static and moving objects [155]. The system efficiently estimated ground surfaces through plane fitting, employing the Random Sample Consensus (RANSAC) algorithm for improved accuracy and robustness. These sensors can precisely detect field boundaries, which is crucial for guiding autonomous agricultural machinery and ensuring smooth operations [155]. This type of sensor is also used to detect static and dynamic obstacles, such as ridges and furrows, in order to ensure safe and effective field operations for autonomous agricultural machinery [72].

A 3D LiDAR was tested for obstacle detection and tracking using point cloud data [72]. The data were processed and clustered with a proposed algorithm, with static obstacles detected through multi-frame fusion and enhanced tracking models. Moving obstacles were tracked using a dynamic tracking point model and a Kalman filter. A LiDAR was tested on an autonomous vehicle, demonstrating that its 3D data accurately represented the environment [156]. In another study, three representation techniques were evaluated: point clouds, feature-based, and grid-based [148]. While point clouds provided high accuracy, they required significant memory and processing power [156]. The feature-based approach relied on recognizable features such as lines, edges, and surfaces [157–159], while the grid-based method divided the area into cells, offering a more memory-efficient and user-friendly solution for sensor data representation in autonomous vehicles [148]. Certain spurious items, such as vegetation and other kinds of clutter, can be more easily recognized and deleted using 3D data, which is one advantage of using LiDAR reference data over ortho-rectified or oblique imagery. In contrast, handling the change in viewpoint and addressing various modalities is necessary when matching imagery to aerial LiDAR. However, it takes longer processing times to recover 3D information from imagery, and the uniformity of the 3D point clouds obtained is not guaranteed because of the lack of texture and detail in large regions. Using stereo methods to recover 3D data from imagery can potentially provide accurate, textured 3D data [160]. LiDAR-derived 3D object detection algorithms are divided into three categories: projection, voxel, and point-based methods. These algorithms have certain limitations. For instance, the view projection algorithm inherently leads to a loss of depth information during projection, as the perceived size of objects depends on their distance from the scanner. Furthermore, objects may become partially or fully occluded in the front view (FV) map, complicating accurate representation. For bird's-eye view (BEV) projection point cloud representation, there are also some limitations, such as small effective areas and sparse representation in BEV maps. Another limitation of BEV projection algorithms is handling occlusion in vertical space, such as handling objects with few points after BEV projection and hand-crafted height features, which may cause information loss with the accumulation of height prediction errors by ground plane fluctuations. The voxel-based view presentation algorithm has information loss limitations during voxelization due to having multiple points in one voxel during the merging. Moreover, the computational cost and cubic memory increase during

the voxel revolution, making voxel-based model training infeasible with high-resolution inputs. Similarly, the point-set algorithm of point cloud representation has limitations of random memory access for feature generation according to the point [161].

Ridge detection in agriculture using this sensor has been widely researched, demonstrating its effectiveness in precision agriculture and autonomous farming. With the 360° field of view, it can comprehensively scan and detect objects such as ridges and field boundaries [19]. In autonomous agricultural machines, its 3D mapping capabilities allow for the accurate detection of crop ridges. Using a laser light for topographic mapping provides detailed terrain representation [162,163]. Ridge detection involves identifying ridge lines from point cloud data, which is commonly used in geospatial applications such as terrain mapping and slope analysis. This process includes filtering point cloud data to separate ground from non-ground points [164,165].

Algorithms such as ridge extraction have been applied to LiDAR data to extract ridgelines in order to create digital representations of terrain ridges for further analysis and mapping [166]. This measures distances with laser pulses, generating 3D point clouds for precise ridge location [167]. The application of LiDAR in challenging environments involves mapping, noise filtering, and machine learning techniques to detect ridges from the point cloud [168]. This technique identifies elevated ridges by creating a 3D point cloud and extracting ridges as separate objects by focusing on the highest points [167]. LiDAR point cloud data have been combined with different machine learning algorithms, such as Random Forest (RF) and Support Vector Machines (SVMs), which can be utilized to classify ridges and furrows accurately or to detect vegetation, roads, and buildings [169]. For ridge extraction, the point cloud data of this sensor were converted into 2D images using morphological operations and edge detection algorithms, which demonstrated success across various terrain and crop types [170]. Recent advancements include the use of deep learning methods, particularly convolutional neural networks (CNNs), which improved the accuracy and efficiency of ridge classification compared to traditional machine learning approaches [171]. However, the widespread adoption of this sensor for ridge detection remains dependent on cost, accessibility, and quality data acquisition through proper testing, as it requires specialized equipment.

4.2. Obstacle Detection

Increasing obstacle density in agricultural field environments presents significant challenges for existing tracking methods. Obstacle detection in agricultural fields is very important for navigation and agricultural operations using agricultural field machinery, especially for autonomous field machines [172–174]. Agricultural environments are complex and unstructured, with four common types of obstacles: positive obstacles (e.g., trees and poles), negative obstacles (e.g., holes and ditches), moving obstacles (e.g., vehicles and people), and difficult terrain (e.g., slopes and water) [175]. Moreover, obstacle characteristics vary based on crop type, landscape curvature, and other factors, and current agricultural vehicles struggle with accurate detection [175].

LiDAR technology offers a solution by providing real-time obstacle detection in these challenging environments. However, obstacles in agricultural fields, such as moving tools and pedestrians, complicate detection and affect decision-making, increasing the risk of uneven operations and collisions [167,176]. While this 3D sensor has been adopted to address these challenges, current methods often lack precision and affect real-time performance [165,175–178]. Advancing this high-precision, sensor-based detection is crucial for improving intelligent agricultural machinery. This sensor, which consists of a laser transmitter, a laser diode (LD), an avalanche photodiode (APD), a time-to-digital converter (TDC), and signal processing units, can estimate the exact distance of obstacles in real-time, as shown in Figure 5a,b.

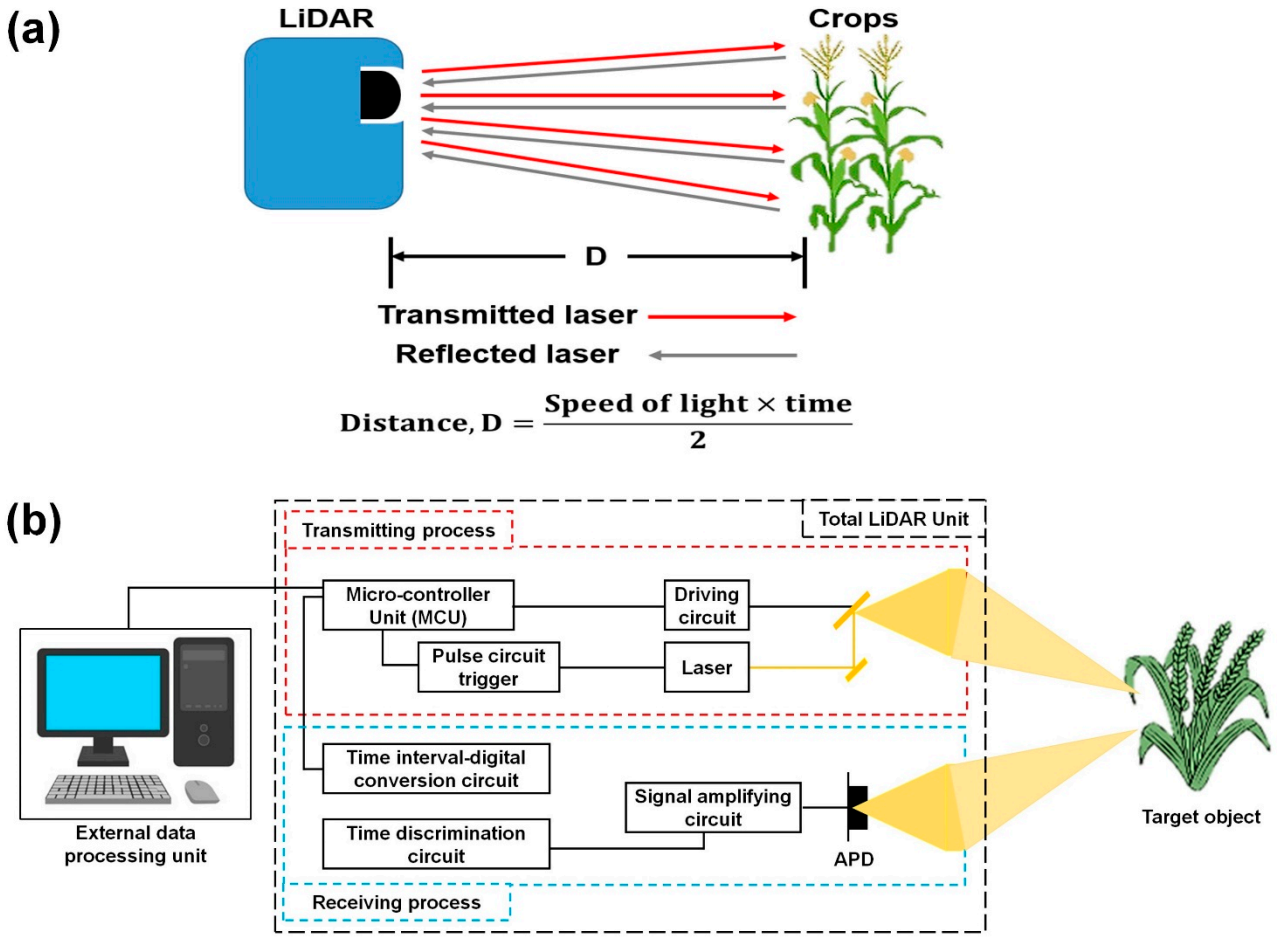

Figure 5. Transmission and reflection of laser from a LiDAR sensor during obstacle detection: (**a**) distance measurement; (**b**) LiDAR sensor components associated with laser transmission and reflection for the measurement of distance.

Despite the existence of various methods and algorithms for object recognition, several limitations remain. A LiDAR system tested under variable conditions and field environments used multiple feature extraction methods, such as average height, density, discontinuity, and connectivity, achieving a 72.4% detection rate with the average height method, while the connectivity method only achieved an 18% detection rate [179]. LiDAR-based obstacle detection typically uses two methods: point cloud clustering and deep learning [73]. Challenges arise from the non-uniform distribution of point clouds, which affects clustering accuracy, and earlier approaches struggled with under-segmentation due to fixed thresholds [173,180,181]. Therefore, several improved algorithms, such as enhancements of the DBSCAN and K-nearest neighbors approach, aimed to tackle under-segmentation but faced challenges with accuracy and real-time performance [180,182]. Recent advancements integrating deep learning techniques such as PointNet, PointPillars, and PointConv aim to improve both accuracy and real-time performance in LiDAR-based obstacle detection [176,183,184].

LiDAR-based obstacle tracking involves two key stages: obstacle data association and obstacle motion state estimation [185]. Muresan et al. [186] used Euclidean distance for data association by computing overlapping regions, while a graph neural network (GNN)-based multi-feature association method improved accuracy but required extensive target knowledge and had high computational demands [85,180]. For motion state estimation, Kalman and extended Kalman filters (EKFs) were applied for multi-target position estimation [187,188]. Convolutional neural network (CNN), multiple hypothesis (MH), and

extended Kalman filter (EKF) methods were used for obstacle detection, data association, and vehicle pose estimation, but accuracy issues persisted [189,190].

To improve agricultural machinery operations, a grid-based obstacle detection and tracking method was proposed [73], showing a 4.86% improvement in detection accuracy and a 47.8% reduction in processing time compared to DBSCAN, with less than 5% tracking error for moving obstacles [73]. A LiDAR mounted on a tractor achieved a detection rate of 72.4% for the average height method and 18% for the connectivity method [180]. Additionally, Asvadi et al. [72] proposed an environment representation architecture that estimated ground surfaces and detected static and moving obstacles above ground level, as illustrated in Figure 6a,b.

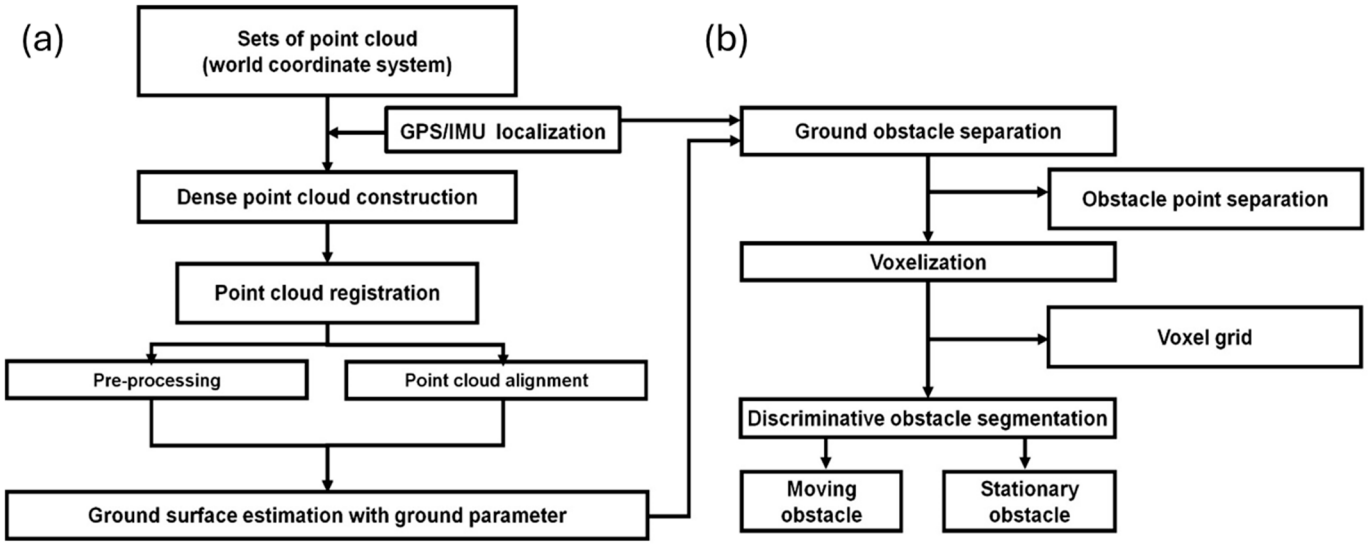

Figure 6. System architecture: (**a**) ground surface elimination; (**b**) detection of static and dynamic obstacles (modified from [72]).

A study proposed using deep learning for obstacle detection in agricultural environments with LiDAR, addressing the limitations of existing methods, which are time-consuming, labor-intensive, and lack generalization [172]. A LiDAR emitting 16 laser beams, each providing both distance and reflectivity data, was used with a vertical field of view of 30° and a horizontal field of view of 360° to detect the agricultural working environment [190]. The study used focal voxel R-CNN methods, which significantly improved the detection of small objects compared to standard voxel R-CNN methods. A method for ground object detection using a downward-pointing angle on a vehicle-mounted LiDAR system was proposed, with data processed through the cascade method [191,192]. The 3D LiDAR predicted height differences to generate an elevation map, introducing three object recognition principles: voxel within a surface, voxel intersecting two surfaces, and voxel at the intersection of three non-parallel surfaces. Despite challenges in crop recognition and obstacle detection, LiDAR sensors showed satisfactory results when mounted on agricultural machinery. Table 3 summarizes various studies and applications of LiDAR sensors for agricultural working environment recognition. The ability of LiDAR to operate effectively in varying weather and light conditions further enhances its utility for working environment recognition, as it remains reliable in low-light, fog, or shadowed areas where other sensors may struggle. Figure 7 shows the schematic diagram of LiDAR usage in agricultural machinery for field crop scanning.

Table 3. Summary of agricultural working environment recognition using different LiDAR sensors.

Parameter	Crop	Method/Algorithm	Conditions	Accuracy (%)	Reference
Obstacle detection	-	Focal voxel R-CNN	Farmland environment	92.89	[172]
	Hay, oats, soybeans, wheat	The density and average height method	Field	49.4; 72.4	[173]
	Corn	Machine vision systems; the average height method	Field	69.5	[174]
	Maize	Classification algorithm	Field	86.5–88.8	[175]
	Trees, bushes	Geometry-based classifier (short baseline and long baseline)	Field	86.5–88.8	[175]
	Wheat	Preprocessing for region of interest, median filtering, DBSCAN clustering	Field	96.67	[193]
Ridge detection	Trees	Mainstream filtering algorithm, digital elevation model (DEM), digital surface model (DSM)	-	99.2	[168]
	-	Euclidean clustering and linear least-squares line fitting, RANSAC line fitting, furrow recognition algorithm	Field	86	[37]
	Paddy	Digital elevation model (DEM)	Field	>96	[193]
	Cauliflower	Filtering of each LiDAR scan, extraction of candidate points caused by furrows, furrow selection using spatiotemporal information of the candidates, and furrow line selection	Field	90	[194]

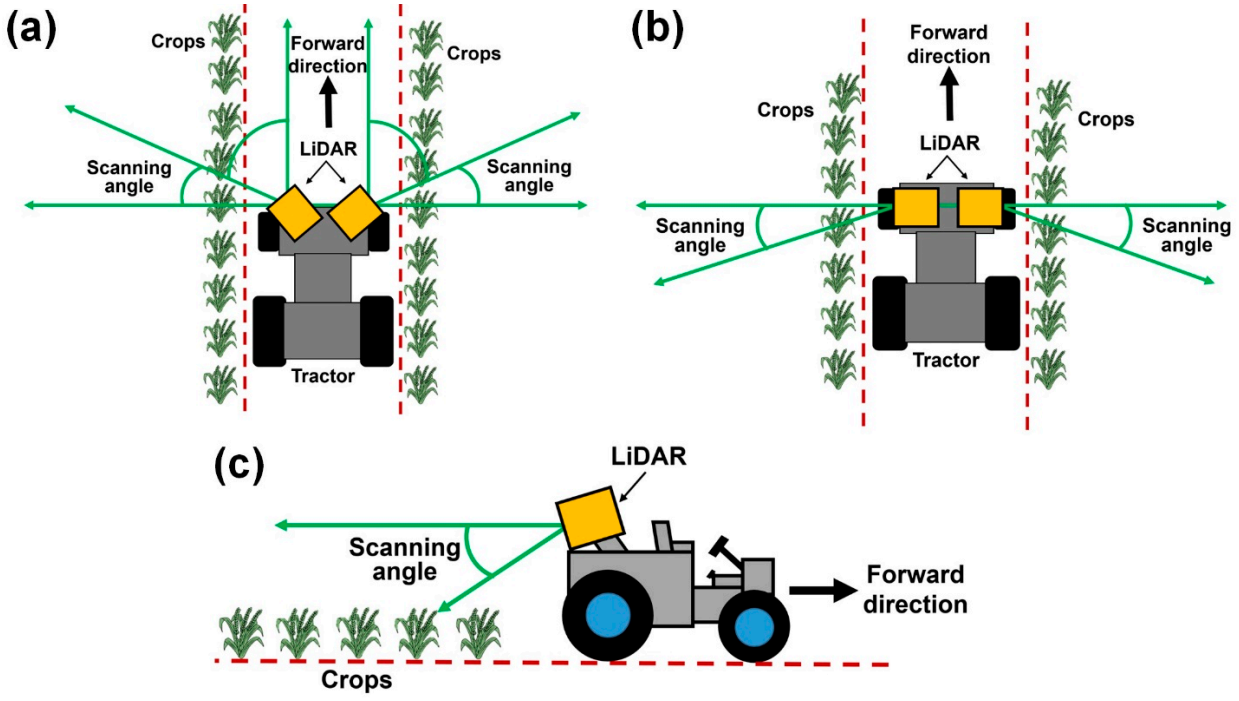

Figure 7. Schematic diagram of application of LiDAR using agricultural machinery: (**a**) front scanning, (**b**) side scanning, and (**c**) back scanning.

5. LiDAR Performance Testing Procedures

LiDAR technology has become increasingly vital in agriculture, offering precise, real-time data for tasks such as crop monitoring, field mapping, and obstacle detection. However, to ensure the accuracy, reliability, and effectiveness of LiDAR sensors in diverse agricultural environments, thorough testing procedures are essential. Agricultural settings present unique challenges, such as varying crop types, uneven terrain, fluctuating weather conditions, and the presence of both static and dynamic obstacles, such as trees, furrows, ditches, and machinery. LiDAR sensors must be rigorously evaluated to confirm their performance in these conditions, ensuring that they meet the demands of precision agriculture. Testing procedures typically assess parameters such as field of view, angular resolution, sensor range, and the impact of environmental factors such as sunlight, moisture, and dust [195,196]. Additionally, the testing of LiDAR in agricultural applications often includes evaluations under dynamic conditions, simulating real-world scenarios encountered by autonomous farming equipment and machinery. By employing structured testing methodologies, LiDAR sensors can be optimized for enhanced data accuracy and operational efficiency, supporting their broader adoption in modern agricultural systems.

Several testing procedures have been proposed in the literature, aiming to evaluate LiDAR sensors' performance under dynamic driving conditions, adverse weather, and varying environmental factors. Proposed methods include unsupervised learning for feature extraction from point clouds, sensor validation in dynamic scenes, and evaluation in controlled environments. In tests simulating harsh conditions using real road fleet data and dynamic test cases, the results showed that environmental factors such as sunlight, reflectivity, and contamination can degrade LiDAR sensors' performance [197,198]. LiDAR test standards are essential to ensure that LiDAR sensors and systems meet the necessary performance benchmarks to deliver accurate, reliable results across a range of applications. These standards, developed by national and international organizations, establish guidelines for the performance, safety, and environmental durability of LiDAR systems. Summarized in [64,199], some key LiDAR testing standards are outlined:

- NHTSA Performance Specifications: The National Highway Traffic Safety Administration (NHTSA) [200] has established minimum performance specifications and test procedures for LiDAR devices. These guidelines set a baseline for acceptable LiDAR performance, particularly for speed measurement devices. These specifications ensure that LiDAR systems meet the accuracy and reliability standards required for legal and operational use in monitoring works;
- SPIE Lidar Data Standardization Tests: The International Society for Optical Instruments (SPIE) [201] helped in the standardization of LiDAR data collection, processing, and analysis. The standardized tests for automotive LiDAR aim to unify the methods used to evaluate LiDAR performance, ensuring consistency across data collection and interpretation in the automotive industry. These tests help align global practices in automotive LiDAR applications;
- USGS Lidar Base Specification: The U.S. Geological Survey (USGS) [202] has developed a LiDAR base specification for the production and quality control of LiDAR data. This specification is widely used within the 3D Elevation Program (3DEP) and serves as a guide for ensuring the quality, accuracy, and compatibility of LiDAR data across a wide range of geospatial applications; it covers data processing practices without dictating specific tools or workflows, allowing flexibility in how data are managed while maintaining strict quality standards;
- DIN-SAE Standard for Automotive LiDAR Performance Testing: The German Institute for Standards (DIN) [203,204] and the Society of Automotive Engineers (SAE) [205] collaborated to develop standardized guidelines for automotive LiDAR performance testing. This standard provides uniform specifications for sensor performance, such as accuracy, range, and field of view, specifically in automotive contexts. These guidelines ensure that LiDAR sensors used in vehicles meet the requirements for safe and reliable operation under real-world conditions;

- Environmental Testing: Environmental durability is a critical aspect of LiDAR sensor testing, especially for outdoor applications in extreme conditions. Temperature testing, for instance, evaluates LiDAR devices under operating conditions ranging from −30 °C (−22 °F) to +60 °C (+140 °F), with relative humidity of up to 90% at 37 °C for extended periods [198,206]. These tests are crucial for ensuring that LiDAR sensors can function accurately under harsh environmental conditions, including in agricultural and automotive applications;
- IEC 60529 Test Standard: The IEC 60529 standard [77] sets guidelines for temperature (15 °C to 35 °C), relative humidity (25% to 75%), and barometric pressure (86 kPa to 106 kPa) in testing LiDAR devices. An International Organization for Standardization (ISO) working group on LiDAR standardization includes world-leading companies such as Valeo, Denso, Bosch, Sony, Nissan, Renault, and ZF. This group focuses on creating global standards for LiDAR technology in automotive and industrial applications, aiming to ensure consistent quality, performance, and safety across different sectors;
- Hesai Testing Standards: Hesai [207,208], a leading LiDAR manufacturer, has developed its own set of testing standards, such as UL4700, GB/T, and ISO/PWI 13228. These standards are used to evaluate LiDAR products for short-, medium-, and long-range applications, focusing on key performance metrics such as detection range, resolution, interference cancellation, and reliability. These standards ensure that LiDAR sensors meet industry-leading requirements and can perform in a wide range of conditions.

LiDAR trials and testing procedures evaluate a variety of performance metrics, including detection range, distance accuracy, angular resolution, field of view, reflectivity, frames per second, and operational safety [64]. Tests also assess the ability of sensors to reject interference, point cloud density, frame delay, and ghost imaging. LiDAR sensors designed to meet international standards and certified by third-party bodies are known as "safety sensors" or "safety laser scanners" [209]. To be certified as such, LiDAR sensors must comply with international safety standards such as ISO 13849 (JIS B9705) Category 3 PLd, IEC 61508 (JIS C 0508) SIL2, and IEC 61496 (JIS B 9704) Type 3 [210]. These certifications ensure the safe application of LiDAR sensors in different applications.

LiDAR testing accuracy is dependent on criteria such as range accuracy, point density, precision, field of view, angular resolution, environmental factors, and system noise [211]. The 3D occupancy grid method was highly effective for tree canopy volume estimation, with the segmented convex hull outperforming the convex hull by 42%, while the cylinder-based model and convex hull methods were faster, with fewer data points, reducing the data usage by 80–100%. No significant differences were observed in treetop volume estimation [64]. Rigorous testing procedures based on industry standards are important for ensuring the accuracy, reliability, and performance of LiDAR sensors in diverse agricultural environments. These tests evaluate key performance metrics such as range accuracy, point density, and environmental resilience.

6. Conclusions

This review highlights the significant benefits of LiDAR technology in agriculture, including the ability to provide precise real-time data for tasks such as crop monitoring, field mapping, and obstacle detection; however, it also addresses some limitations, such as the impact of environmental conditions, cost concerns, and the need for reliable data processing algorithms. In this paper, the future directions for the application of LiDAR in agriculture are further outlined, emphasizing the need for continual advancements in sensor technology and the integration of complementary systems, such as machine learning, for improved performance and accuracy.

LiDAR sensor testing procedures are also discussed in this review, focusing on critical testing parameters, industry standards, and accuracy benchmarks; it explores the technical specifications of several commercially available LiDAR sensors and emphasizes the im-

portance of mounting LiDAR technology on agricultural field machinery for the effective recognition of crops and working environments. This study underscores that achieving high-quality 3D point cloud data from LiDAR sensors requires adhering to proper testing procedures and standards throughout the testing process. LiDAR sensors have achieved high levels of accuracy in tasks such as tree recognition, plant height estimation, and canopy volume calculation, making them invaluable tools for precision agriculture. The continuous development of and adherence to standardized testing methods will further enhance the capabilities and adoption of LiDAR systems in modern agricultural practice.

This review found that LiDAR sensors are popular for their 360° field of view, high accuracy, and precise data collection despite challenges related to illuminance, weather conditions, and temperature. Based on field test results from multiple researchers and findings from reviewed articles, LiDAR is considered to be a highly precise sensing technology for crop detection and recognition in agricultural environments. The reviewed studies suggest certain specific guidelines during the testing of LiDAR to ensure optimal performance and reliability. Proper calibration of LiDAR equipment should be ensured in order to accurately measure and detect features in the agricultural working environment. Comprehensive field tests across diverse crops and environments need to be conducted to evaluate the performance of LiDAR under varying conditions, and the results should be analyzed to assess detection precision and identify potential limitations or areas for improvement. To refine the accuracy of LiDAR systems, repeated testing is necessary to ensure that they operate at their full potential. The incorporation of additional technologies or algorithms alongside LiDAR should be considered in order to enhance overall system performance and accuracy. Advanced data processing algorithms could be used to reduce processing times for point cloud data and improve sensor efficiency.

In this review, we suggest utilizing affordable electronic components due to their lower costs, making LiDAR technology more accessible for the recognition of crops and agricultural operational environments, along with the autonomous navigation of agricultural field machinery. A thorough evaluation of the accuracy and reliability of LiDAR sensors should be carried out in real field conditions, as also suggested in this study. A strategic framework for the effective implementation of LiDAR technology in diverse farming environments is offered in this review, which includes recommendations for improved testing procedures, suggestions for addressing current limitations, and guidance on integrating LiDAR with other technologies to enhance its potential in precision agriculture. The study concluded that LiDAR can become a more accessible and valuable tool for modern farming by following these guidelines, supporting the future of smart agriculture with autonomous farming systems.

Author Contributions: Conceptualization, M.R.K. and S.-O.C.; methodology, M.R.K. and S.-O.C.; software, M.R.K. and M.N.R.; validation, M.R.K., M.N.R., H.J., M.A.H., K.-H.L. and J.S.; formal analysis, M.R.K., M.N.R., H.J. and M.A.H.; investigation, J.S. and S.-O.C.; resources, S.-O.C.; data curation, H.J., M.N.R., M.A.H., K.-H.L. and J.S.; writing—original draft preparation, M.R.K.; writing—review and editing, M.R.K., M.N.R., K.-H.L., J.S. and S.-O.C.; visualization, M.R.K., K.-H.L. and J.S.; supervision, S.-O.C.; project administration, S.-O.C.; funding acquisition, S.-O.C. All authors have read and agreed to the published version of the manuscript.

Funding: This work was supported by Korea Institute of Planning and Evaluation for Technology in Food, Agriculture and Forestry (IPET), through the Open Field Smart Agriculture Technology Short-term Advancement Program, funded by Ministry of Agriculture, Food and Rural Affairs (MAFRA) (Project No. RS-2022-IP322029), Republic of Korea.

Data Availability Statement: Not applicable.

Conflicts of Interest: Dr. Joonjea Sung's affiliation with FYD Company Ltd., Suwon 16676, Republic of Korea, does not influence the content or outcomes of this research. The other authors declare no conflicts of interest.

References

1. Daszkiewicz, T. Food production in the context of global developmental challenges. *Agriculture* **2022**, *12*, 832. [CrossRef]
2. Barrett, C.B. Overcoming global food security challenges through science and solidarity. *Am. J. Agric. Econ.* **2021**, *103*, 422–447. [CrossRef]
3. Pachapur, P.K.; Pachapur, V.L.; Brar, S.K.; Galvez, R.; Le Bihan, Y.; Surampalli, R.Y. Food security and sustainability. In *Sustainability: Fundamentals and Applications*; Wiley: Hoboken, NJ, USA, 2020; pp. 357–374.
4. Morchid, A.; El Alami, R.; Raezah, A.A.; Sabbar, Y. Applications of Internet of Things (IoT) and sensors technology to increase food security and agricultural sustainability: Benefits and challenges. *Ain Shams Eng. J.* **2023**, *15*, 102509. [CrossRef]
5. Rivera, G.; Porras, R.; Florencia, R.; Sánchez-Solís, J.P. LiDAR applications in precision agriculture for cultivating crops: A review of recent advances. *Comput. Electron. Agric.* **2023**, *207*, 107737. [CrossRef]
6. Farhan, S.M.; Yin, J.; Chen, Z.; Memon, M.S. A Comprehensive Review of LiDAR Applications in Crop Management for Precision Agriculture. *Sensors* **2024**, *24*, 5409. [CrossRef]
7. Wang, X.; Pan, H.; Guo, K.; Yang, X.; Luo, S. The evolution of LiDAR and its application in high precision measurement. *IOP Conf. Ser Earth Environ. Sci.* **2020**, *502*, 012008. [CrossRef]
8. Ahmed, S.A.; Mohsin, M.; Ali, S.M.Z. Survey and technological analysis of laser and its defense applications. *Def. Technol.* **2021**, *17*, 583–592. [CrossRef]
9. Ji, Q.; Zong, S.; Yang, J. Application and development trend of laser technology in military field. In Proceedings of the ICOSM 2020: Optoelectronic Science and Materials, Hefei, China, 25–27 September 2020; Volume 11606, pp. 32–40.
10. Jones, L.; Hobbs, P. The application of terrestrial LiDAR for geohazard mapping, monitoring and modelling in the British Geological Survey. *Remote Sens.* **2021**, *13*, 395. [CrossRef]
11. Sakib, S.M. LiDAR Technology—An Overview. *IUP J. Electr. Electron. Eng.* **2022**, *15*, 36.
12. Li, N.; Ho, C.P.; Xue, J.; Lim, L.W.; Chen, G.; Fu, Y.H.; Lee, L.Y.T. A progress review on solid-state LiDAR and nanophotonics-based LiDAR sensors. *Laser Photonics Rev.* **2022**, *16*, 2100511. [CrossRef]
13. Wang, C.; Yang, X.; Xi, X.; Nie, S.; Dong, P. LiDAR Remote Sensing Principles. In *Introduction to LiDAR Remote Sensing*; Taylor & Francis: Abingdon, UK, 2024.
14. Guo, Q.; Su, Y.; Hu, T. *LiDAR Principles, Processing and Applications in Forest Ecology*; Academic Press: Cambridge, MA, USA, 2023.
15. Xiang, L.; Wang, D. A review of three-dimensional vision techniques in food and agriculture applications. *Smart Agric. Technol.* **2023**, *5*, 100259. [CrossRef]
16. Debnath, S.; Paul, M.; Debnath, T. Applications of LiDAR in agriculture and future research directions. *J. Imaging.* **2023**, *9*, 57. [CrossRef] [PubMed]
17. Bilik, I. Comparative analysis of radar and lidar technologies for automotive applications. *IEEE Intell. Transp. Syst. Mag.* **2022**, *15*, 244–269. [CrossRef]
18. Omia, E.; Bae, H.; Park, E.; Kim, M.S.; Baek, I.; Kabenge, I.; Cho, B.K. Remote sensing in field crop monitoring: A comprehensive review of sensor systems, data analyses and recent advances. *Remote Sens.* **2023**, *15*, 354. [CrossRef]
19. Borowiec, N.; Marmol, U. Using LiDAR system as a data source for agricultural land boundaries. *Remote Sens.* **2022**, *14*, 1048. [CrossRef]
20. Yuan, H.; Bennett, R.S.; Wang, N.; Chamberlin, K.D. Development of a peanut canopy measurement system using a ground-based LiDAR sensor. *Front. Plant Sci.* **2019**, *10*, 203. [CrossRef]
21. Karunathilake, E.M.B.M.; Le, A.T.; Heo, S.; Chung, Y.S.; Mansoor, S. The path to smart farming: Innovations and opportunities in precision agriculture. *Agriculture* **2023**, *13*, 1593. [CrossRef]
22. Sishodia, R.P.; Ray, R.L.; Singh, S.K. Applications of remote sensing in precision agriculture: A review. *Remote Sens.* **2020**, *12*, 3136. [CrossRef]
23. Jin, S.; Sun, X.; Wu, F.; Su, Y.; Li, Y.; Song, S.; Guo, Q. Lidar sheds new light on plant phenomics for plant breeding and management: Recent advances and future prospects. *ISPRS J. Photogramm. Remote Sens.* **2021**, *171*, 202–223. [CrossRef]
24. Zhou, L.; Gu, X.; Cheng, S.; Yang, G.; Shu, M.; Sun, Q. Analysis of plant height changes of lodged maize using UAV-LiDAR data. *Agriculture* **2020**, *10*, 146. [CrossRef]
25. Nidamanuri, R.R. Deep learning-based prediction of plant height and crown area of vegetable crops using LiDAR point cloud. *Sci. Rep.* **2024**, *14*, 14903.
26. Wang, J.; Zhang, Y.; Gu, R. Research status and prospects on plant canopy structure measurement using visual sensors based on three-dimensional reconstruction. *Agriculture* **2020**, *10*, 462. [CrossRef]
27. Wu, D.; Johansen, K.; Phinn, S.; Robson, A. Suitability of airborne and terrestrial laser scanning for mapping tree crop structural metrics for improved orchard management. *Remote Sens.* **2020**, *12*, 1647. [CrossRef]
28. Zhang, F.; Hassanzadeh, A.; Kikkert, J.; Pethybridge, S.J.; van Aardt, J. Evaluation of Leaf Area Index (LAI) of Broadacre crops using UAS-Based LiDAR point clouds and multispectral imagery. *IEEE J. Sel. Top. Appl. Earth Obs. Remote Sens.* **2022**, *15*, 4027–4044. [CrossRef]
29. Shendryk, Y.; Sofonia, J.; Garrard, R.; Rist, Y.; Skocaj, D.; Thorburn, P. Fine-scale prediction of biomass and leaf nitrogen content in sugarcane using UAV LiDAR and multispectral imaging. *Int. J. Appl. Earth Obs. Geoinf.* **2020**, *92*, 102177. [CrossRef]
30. Neupane, K.; Baysal-Gurel, F. Automatic identification and monitoring of plant diseases using unmanned aerial vehicles: A review. *Remote Sens.* **2021**, *13*, 3841. [CrossRef]

31. Moreno, H.; Andújar, D. Proximal sensing for geometric characterization of vines: A review of the latest advances. *Comput. Electron. Agric.* **2023**, *210*, 107901. [CrossRef]
32. Pagliai, A.; Ammoniaci, M.; Sarri, D.; Lisci, R.; Perria, R.; Vieri, M.; Kartsiotis, S.P. Comparison of aerial and ground 3D point clouds for canopy size assessment in precision viticulture. *Remote Sens.* **2022**, *14*, 1145. [CrossRef]
33. Sinha, R.; Quirós, J.J.; Sankaran, S.; Khot, L.R. High resolution aerial photogrammetry based 3D mapping of fruit crop canopies for precision inputs management. *Inf. Process. Agric.* **2022**, *9*, 11–23. [CrossRef]
34. Shi, J.; Bai, Y.; Diao, Z.; Zhou, J.; Yao, X.; Zhang, B. Row detection BASED navigation and guidance for agricultural robots and autonomous vehicles in row-crop fields: Methods and applications. *Agronomy* **2023**, *13*, 1780. [CrossRef]
35. Padhiary, M.; Kumar, R.; Sethi, L.N. Navigating the Future of Agriculture: A Comprehensive Review of Automatic All-Terrain Vehicles in Precision Farming. *J. Inst. Eng. Ser. A* **2024**, *105*, 767–782. [CrossRef]
36. Kabir, M.M.; Jim, J.R.; Istenes, Z. Terrain detection and segmentation for autonomous vehicle navigation: A state-of-the-art systematic review. *Inf. Fusion* **2025**, *113*, 102644. [CrossRef]
37. Soitinaho, R.; Oksanen, T. Ploughing furrow recognition for onland ploughing using a 3D-LiDAR sensor. *Comput. Electron. Agric.* **2023**, *210*, 107941.
38. Wang, X.; Shu, L.; Han, R.; Yang, F.; Gordon, T.; Wang, X.; Xu, H. A survey of farmland boundary extraction technology based on remote sensing images. *Electronics* **2023**, *12*, 1156. [CrossRef]
39. Chen, W.; Liu, Q.; Hu, H.; Liu, J.; Wang, S.; Zhu, Q. Novel laser-based obstacle detection for autonomous robots on unstructured terrain. *Sensors* **2020**, *20*, 5048. [CrossRef]
40. Zhou, L.; Wang, J.; Lin, S.; Chen, Z. Terrain traversability mapping based on lidar and camera fusion. In Proceedings of the 8th International Conference on Automation, Robotics and Applications (ICARA), Prague, Czech Republic, 18–20 February 2022; pp. 217–222.
41. Lopac, N.; Jurdana, I.; Brnelić, A.; Krljan, T. Application of laser systems for detection and ranging in the modern road transportation and maritime sector. *Sensors* **2022**, *22*, 5946. [CrossRef]
42. Gregersen, E. LiDAR. Encyclopaedia Britannica. Available online: https://www.britannica.com/technology/lidar (accessed on 23 July 2024).
43. Peladarinos, N.; Piromalis, D.; Cheimaras, V.; Tserepas, E.; Munteanu, R.A.; Papageorgas, P. Enhancing smart agriculture by implementing digital twins: A comprehensive review. *Sensors* **2023**, *23*, 7128. [CrossRef]
44. Cao, X.; Liu, Y.; Yu, R.; Han, D.; Su, B. A comparison of UAV RGB and multispectral imaging in phenotyping for stay green of wheat population. *Remote Sens.* **2021**, *13*, 5173. [CrossRef]
45. Holm, S.; Nelson, R.; Ståhl, G. Hybrid three-phase estimators for large-area forest inventory using ground plots, airborne LiDAR, and space LiDAR. *Remote Sens. Environ.* **2017**, *197*, 85–97. [CrossRef]
46. Purcell, W.; Neubauer, T. Digital Twins in Agriculture: A State-of-the-art review. *Smart Agric. Technol.* **2023**, *3*, 100094. [CrossRef]
47. Xiong, J.; Yu, D.; Liu, S.; Shu, L.; Wang, X.; Liu, Z. A review of plant phenotypic image recognition technology based on deep learning. *Electronics* **2021**, *10*, 81. [CrossRef]
48. Darwin, B.; Dharmaraj, P.; Prince, S.; Popescu, D.E.; Hemanth, D.J. Recognition of bloom/yield in crop images using deep learning models for smart agriculture: A review. *Agronomy* **2021**, *11*, 646. [CrossRef]
49. Anand, K.J.; Nagre, S.P.; Shrivastava, M.K.; Amrate, P.K.; Patel, T.; Katara, V.K. Enhancing crop improvement through synergistic integration of advanced plant breeding and proximal remote sensing techniques: A review. *Int. J. Plant Soil Sci.* **2023**, *35*, 121–138. [CrossRef]
50. Ma, Z.; Rayhana, R.; Feng, K.; Liu, Z.; Xiao, G.; Ruan, Y.; Sangha, J.S. A review on sensing technologies for high-throughput plant phenotyping. *IEEE Open J. Instrum. Meas.* **2022**, *1*, 9500121. [CrossRef]
51. Liu, H.; Bruning, B.; Garnett, T.; Berger, B. Hyperspectral imaging and 3D technologies for plant phenotyping: From satellite to close-range sensing. *Comput. Electron. Agric.* **2020**, *175*, 105621. [CrossRef]
52. Feng, L.; Chen, S.; Zhang, C.; Zhang, Y.; He, Y. A comprehensive review on recent applications of unmanned aerial vehicle remote sensing with various sensors for high-throughput plant phenotyping. *Comput. Electron. Agric.* **2021**, *182*, 106033. [CrossRef]
53. Sun, S.; Li, C.; Chee, P.W.; Paterson, A.H.; Meng, C.; Zhang, J.; Ma, P.; Robertson, J.S.; Adhikari, J. High resolution 3D terrestrial LiDAR for cotton plant main stalk and node detection. *Comput. Electron. Agric.* **2021**, *187*, 106276. [CrossRef]
54. Rosell, J.R.; Sanz, R. A review of methods and applications of the geometric characterization of tree crops in agricultural activities. *Comput. Electron. Agric.* **2012**, *81*, 124–141. [CrossRef]
55. Miyake, Y.; Kimoto, S.; Uchiyama, Y.; Kohsaka, R. Income change and inter-farmer relations through conservation agriculture in Ishikawa Prefecture, Japan: Empirical analysis of economic and behavioral factors. *Land* **2022**, *11*, 245. [CrossRef]
56. Awadallah, M.O.M.; Juárez, A.; Alfredsen, K. Comparison between topographic and bathymetric LiDAR terrain models in flood inundation estimations. *Remote Sens.* **2022**, *14*, 227. [CrossRef]
57. Mehendale, N.; Neoge, S. Review on LiDAR technology. *SSRN* **2020**, 3604309.
58. Bates, J.S.; Montzka, C.; Schmidt, M.; Jonard, F. Estimating canopy density parameters time-series for winter wheat using UAS mounted LiDAR. *Remote Sens.* **2021**, *13*, 710. [CrossRef]
59. Schulze-Brüninghoff, D.; Hensgen, F.; Wachendorf, M.; Astor, T. Methods for LiDAR-based estimation of extensive grassland biomass. *Comput. Electron. Agric.* **2019**, *156*, 693–699.

60. Zhang, Z.; Wang, X.; Lai, Q.; Zhang, Z. Review of variable-rate sprayer applications based on real-time sensor technologies. In *Automation in Agriculture-Securing Food Supplies for Future Generations*; InTech: Rijeka, Croatia, 2018; p. 13.
61. Lussem, U.; Bolten, A.; Menne, J.; Gnyp, M.L.; Schellberg, J.; Bareth, G. Estimating biomass in temperate grassland with high resolution canopy surface models from UAV-based RGB images and vegetation indices. *J. Appl. Remote Sens.* **2019**, *13*, 034525. [CrossRef]
62. Zhu, H. Development of UAV-Based Lidar Crop Height Mapping System. Ph.D. Thesis, University of Illinois at Urbana-Champaign, Champaign, IL, USA, 2017.
63. He, C.; Convertino, M.; Feng, Z.; Zhang, S. Using LiDAR data to measure the 3D green biomass of Beijing urban forest in China. *PLoS ONE* **2013**, *8*, 75920. [CrossRef]
64. Selbeck, J.; Dworak, V.; Ehlert, D. Testing a vehicle-based scanning lidar sensor for crop detection. *Can. J. Remote Sens.* **2010**, *36*, 24–35.
65. Rhee, H.; Seo, J. Application of GeoWEPP to determine the annual average sediment yield of erosion control dams in Korea. *Korean J. Agric. Sci.* **2020**, *47*, 803–814.
66. Panjvani, K.; Dinh, A.V.; Wahid, K.A. LiDARPheno—A low-cost LiDAR-based 3D scanning system for leaf morphological trait extraction. *Front. Plant Sci.* **2019**, *10*, 147.
67. Arnó, J.; Escolà, A.; Vallès, J.M.; Llorens, J.; Sanz, R.; Masip, J.; Palacín, J.; Rosell-Polo, J.R. Leaf area index estimation in vineyards using a ground-based LiDAR scanner. *Precis. Agric.* **2013**, *14*, 290–306.
68. Polo, J.R.; Sanz, R.; Llorens, J.; Arnó, J.; Escola, A.; Ribes-Dasi, M.; Masip, J.; Camp, F.; Gràcia, F.; Solanelles, F.; et al. A tractor-mounted scanning LiDAR for the non-destructive measurement of vegetative volume and surface area of tree-row plantations: A comparison with conventional destructive measurements. *Biosyst. Eng.* **2009**, *102*, 128–134.
69. Gené-Mola, J.; Gregorio, E.; Cheein, F.A.; Guevara, J.; Llorens, J.; Sanz-Cortiella, R.; Escolà, A.; Rosell-Polo, J.R. Fruit detection, yield prediction, and canopy geometric characterization using LiDAR with forced air flow. *Comput. Electron. Agric.* **2020**, *168*, 105121. [CrossRef]
70. Guo, Q.; Wu, F.; Pang, S.; Zhao, X.; Chen, L.; Liu, J.; Xue, B.; Xu, G.; Li, L.; Jing, H.; et al. Crop 3D—A LiDAR-based platform for 3D high-throughput crop phenotyping. *Sci. China Life Sci.* **2018**, *61*, 328–339. [CrossRef] [PubMed]
71. Sterenczak, K.; Zasada, M. Accuracy of tree height estimation based on LiDAR data analysis. *Folia For. Polonica Ser. A For.* **2011**, *53*, 123–129.
72. Asvadi, A.; Premebida, C.; Peixoto, P.; Nunes, U. 3D LiDAR-based static and moving obstacle detection in driving environments: An approach based on voxels and multi-region ground planes. *Robot. Auton. Syst.* **2016**, *83*, 299–311. [CrossRef]
73. Jiang, W.; Chen, W.; Song, C.; Yan, Y.; Zhang, Y.; Wang, S. Obstacle detection and tracking for intelligent agricultural machinery. *Comput. Electr. Eng.* **2023**, *108*, 108670. [CrossRef]
74. Foldager, F.F.; Pedersen, J.M.; Haubro Skov, E.; Evgrafova, A.; Green, O. LiDAR-based 3D scans of soil surfaces and furrows in two soil types. *Sensors* **2019**, *19*, 661. [CrossRef]
75. Hu, T.; Su, Y.; Xue, B.; Liu, J.; Zhao, X.; Fang, J.; Guo, Q. Mapping global forest aboveground biomass with spaceborne LiDAR, optical imagery, and forest inventory data. *Remote Sens.* **2016**, *8*, 565. [CrossRef]
76. Iqbal, J.; Xu, R.; Sun, S.; Li, C. Simulation of an autonomous mobile robot for LiDAR-based in-field phenotyping and navigation. *Robotics* **2020**, *9*, 46. [CrossRef]
77. Aguiar, A.S.; Neves dos Santos, F.; Sobreira, H.; Boaventura-Cunha, J.; Sousa, A.J. Localization and mapping on agriculture based on point-feature extraction and semiplanes segmentation from 3D LiDAR data. *Front. Robot. AI* **2022**, *9*, 14. [CrossRef]
78. Choudhary, A.; Kobayashi, Y.; Arjonilla, F.J.; Nagasaka, S.; Koike, M. Evaluation of mapping and path planning for non-holonomic mobile robot navigation in narrow pathway for agricultural application. In Proceedings of the 2021 IEEE/SICE International Symposium on System Integration (SII), Narvik, Norway, 11–14 January 2021; pp. 17–22.
79. Emmi, L.; Le Flécher, E.; Cadenat, V.; Devy, M. A hybrid representation of the environment to improve autonomous navigation of mobile robots in agriculture. *Precis. Agric.* **2021**, *22*, 524–549. [CrossRef]
80. Koenig, K.; Höfle, B.; Hämmerle, M.; Jarmer, T.; Siegmann, B.; Lilienthal, H. Comparative classification analysis of post-harvest growth detection from terrestrial LiDAR point clouds in precision agriculture. *ISPRS J. Photogramm. Remote Sens.* **2015**, *104*, 112–125. [CrossRef]
81. Kragh, M.; Jorgensen, R.N.; Pedersen, H. Object detection and terrain classification in agricultural fields using 3D LiDAR data. In Proceedings of the 10th International Conference on Computer Vision Systems (ICVS), Copenhagen, Denmark, 6–9 July 2015; pp. 188–197.
82. Kragh, M.; Underwood, J. Multimodal obstacle detection in unstructured environments with conditional random fields. *J. Field Robot.* **2020**, *37*, 53–72. [CrossRef]
83. Jayakumari, R.; Nidamanuri, R.R.; Ramiya, A.M. Object-level classification of vegetable crops in 3D LiDAR point cloud using deep learning convolutional neural networks. *Precis. Agric.* **2021**, *22*, 1617–1633. [CrossRef]
84. Su, Y.; Wu, F.; Ao, Z.; Jin, S.; Qin, F.; Liu, B.; Pang, S.; Liu, L.; Guo, Q. Evaluating maize phenotype dynamics under drought stress using terrestrial LiDAR. *Plant Methods* **2019**, *15*, 11. [CrossRef]
85. Wu, S.; Wen, W.; Xiao, B.; Guo, X.; Du, J.; Wang, C.; Wang, Y. An accurate skeleton extraction approach from 3D point clouds of maize plants. *Front. Plant Sci.* **2019**, *10*, 248. [CrossRef]

86. Wang, K.; Zhou, J.; Zhang, W.; Zhang, B. Mobile LiDAR scanning system combined with canopy morphology extracting methods for tree crown parameters evaluation in orchards. *Sensors* **2021**, *21*, 339. [CrossRef]
87. Zhou, M.; Jiang, H.; Bing, Z.; Su, H.; Knoll, A. Design and evaluation of the target spray platform. *Int. J. Adv. Robot. Syst.* **2021**, *18*, 1729881421996146. [CrossRef]
88. Wang, R.; Peethambaran, J.; Chen, D. LiDAR point clouds to 3-D urban models: A review. *IEEE J. Sel. Top. Appl. Earth Obs. Remote Sens.* **2018**, *11*, 606–627. [CrossRef]
89. Liu, K.; Dong, X.Y.; Qiu, B.J. Analysis of cotton height spatial variability based on UAV-LiDAR. *Precis. Agric. Aviat.* **2020**, *3*, 72–76. [CrossRef]
90. Zhang, C.; Craine, W.A.; McGee, R.J.; Vandemark, G.J.; Davis, J.B.; Brown, J.; Hulbert, S.H.; Sankaran, S. High-throughput phenotyping of canopy height in cool-season crops using sensing techniques. *Agron. J.* **2021**, *113*, 3269–3280. [CrossRef]
91. Cassidy, R.; Thomas, I.A.; Higgins, A.; Bailey, J.S.; Jordan, P. A carrying capacity framework for soil phosphorus and hydrological sensitivity from farm to catchment scales. *Sci. Total Environ.* **2019**, *687*, 277–286. [CrossRef] [PubMed]
92. Florent, D.; Bernadett, G.; Janos, T.; Imri, D.; Attila, N. Evaluation of soil water management properties based on LiDAR data and soil analyses, at farm level. *Nat. Resour. Sustain. Dev.* **2019**, *9*, 160–173.
93. Dhami, H.; Yu, K.; Xu, T.; Zhu, Q.; Dhakal, K.; Friel, J.; Li, S.; Tokekar, P. Crop height and plot estimation for phenotyping from unmanned aerial vehicles using 3D LiDAR. In Proceedings of the 2020 IEEE/RSJ International Conference on Intelligent Robots and Systems (IROS), Las Vegas, NV, USA, 25–29 October 2020; pp. 2643–2649.
94. Wu, L.; Zhu, X.; Lawes, R.; Dunkerley, D.; Zhang, H. Comparison of machine learning algorithms for classification of LiDAR points for characterization of canola canopy structure. *Int. J. Remote Sens.* **2019**, *40*, 5973–5991. [CrossRef]
95. Ivushkin, K.; Bartholomeus, H.; Bregt, A.K.; Pulatov, A.; Franceschini, M.H.; Kramer, H.; van Loo, E.N.; Roman, V.J.; Finkers, R. UAV based soil salinity assessment of cropland. *Geoderma* **2019**, *338*, 502–512. [CrossRef]
96. Maimaitijiang, M.; Sagan, V.; Erkbol, H.; Adrian, J.; Newcomb, M.; LeBauer, D.; Pauli, D.; Shakoor, N.; Mockler, T.C. UAV-based sorghum growth monitoring: A comparative analysis of LiDAR and photogrammetry. *ISPRS Ann. Photogramm. Remote Sens. Spat. Inf. Sci.* **2020**, *3*, 489. [CrossRef]
97. Sofonia, J.; Shendryk, Y.; Phinn, S.; Roelfsema, C.; Kendoul, F.; Skocaj, D. Monitoring sugarcane growth response to varying nitrogen application rates: A comparison of UAV SLAM LiDAR and photogrammetry. *Int. J. Appl. Earth Obs. Geoinf.* **2019**, *82*, 101878. [CrossRef]
98. Itakura, K.; Hosoi, F. Automatic individual tree detection and canopy segmentation from three-dimensional point cloud images obtained from ground-based LiDAR. *J. Agric. Meteorol.* **2018**, *74*, 109–113. [CrossRef]
99. George, R.M.; Barrett, B.A.; Ghamkhar, K.; Whyatt, J. Evaluation of LiDAR scanning for measurement of yield in perennial ryegrass. *N. Z. Grassl.* **2019**, *81*, 55–60. [CrossRef]
100. Ziliani, M.G.; Parkes, S.D.; Hoteit, I.; McCabe, M.F. Intra-season crop height variability at commercial farm scales using a fixed-wing UAV. *Remote Sens* **2018**, *10*, 2007. [CrossRef]
101. Yuan, W.; Li, J.; Bhatta, M.; Shi, Y.; Baenziger, P.S.; Ge, Y. Wheat height estimation using LiDAR in comparison to ultrasonic sensor and UAS. *Sensors* **2018**, *18*, 3731. [CrossRef]
102. Vidoni, R.; Gallo, R.; Ristorto, G.; Carabin, G.; Mazzetto, F.; Scalera, L.; Gasparetto, A. ByeLab: An agricultural mobile robot prototype for proximal sensing and precision farming. *ASME Int. Mech. Eng. Congr. Expo.* **2017**, *4*, 58370.
103. Sun, S.; Li, C.; Paterson, A.H.; Jiang, Y.; Xu, R.; Robertson, J.S.; Snider, J.L.; Chee, P.W. In-field high throughput phenotyping and phenotype data analysis for cotton plant growth using LiDAR. *Front. Plant Sci.* **2018**, *9*, 16. [CrossRef] [PubMed]
104. Escolà, A.; Martínez-Casasnovas, J.A.; Rufat, J.; Arnó, J.; Arbonés, A.; Sebé, F.; Pascual, M.; Gregorio, E.; Rosell-Polo, J.R. Mobile terrestrial laser scanner applications in precision fruiticulture/horticulture and tools to extract information from canopy point clouds. *Precis. Agric.* **2017**, *18*, 111–132. [CrossRef]
105. Ghamkhar, K.; Irie, K.; Hagedorn, M. Real-time, non-destructive and in-field foliage yield and growth rate measurement in perennial ryegrass (*Lolium perenne* L.). *Plant Methods* **2019**, *15*, 72. [CrossRef] [PubMed]
106. Karim, M.R.; Ahmed, S.; Reza, M.N.; Lee, K.-H.; Jin, H.; Ali, M.; Chung, S.-O.; Sung, J. A review on stereo vision for feature characterization of upland crops and orchard fruit trees. *Precis. Agric.* **2024**, *6*, 104–122.
107. Bicamumakuba, E.; Habineza, E.; Lee, K.-H.; Chung, S.-O. Sensor technologies for remote monitoring of automated orchard irrigation: A review. *Precis. Agric.* **2024**, *6*, 81–95.
108. Pérez-Harguindeguy, N.; Díaz, S.; Garnier, E.; Lavorel, S.; Poorter, H.; Jaureguiberry, P.; Bret-Harte, M.S.; Cornwell, W.K.; Craine, J.M.; Gurvich, D.E.; et al. Corrigendum to: New handbook for standardised measurement of plant functional traits worldwide. *Aust. J. Bot.* **2016**, *64*, 715–716. [CrossRef]
109. Bhatta, M.; Eskridge, K.M.; Rose, D.J.; Santra, D.K.; Baenziger, P.S.; Regassa, T. Seeding rate, genotype, and topdressed nitrogen effects on yield and agronomic characteristics of winter wheat. *Crop Sci.* **2017**, *57*, 951–963. [CrossRef]
110. Sadeghi-Tehran, P.; Virlet, N.; Sabermanesh, K.; Hawkesford, M.J. Multi-feature machine learning model for automatic segmentation of green fractional vegetation cover for high-throughput field phenotyping. *Plant Methods* **2017**, *13*, 103. [CrossRef]
111. Yue, J.; Yang, G.; Li, C.; Li, Z.; Wang, Y.; Feng, H.; Xu, B. Estimation of winter wheat above-ground biomass using unmanned aerial vehicle-based snapshot hyperspectral sensor and crop height improved models. *Remote Sens.* **2017**, *9*, 708. [CrossRef]
112. Lau, A.; Bentley, L.P.; Martius, C.; Shenkin, A.; Bartholomeus, H.; Raumonen, P.; Malhi, Y.; Jackson, T.; Herold, M. Quantifying branch architecture of tropical trees using terrestrial LiDAR and 3D modelling. *Trees* **2018**, *32*, 1219–1231. [CrossRef]

113. Jimenez-Berni, J.A.; Deery, D.M.; Rozas-Larraondo, P.; Condon, A.T.G.; Rebetzke, G.J.; James, R.A.; Bovill, W.D.; Furbank, R.T.; Sirault, X.R. High throughput determination of plant height, ground cover, and above-ground biomass in wheat with LiDAR. *Front. Plant Sci.* **2018**, *9*, 237. [CrossRef] [PubMed]
114. Qiu, Q.; Sun, N.; Bai, H.; Wang, N.; Fan, Z.; Wang, Y.; Meng, Z.; Li, B.; Cong, Y. Field-based high-throughput phenotyping for maize plant using 3D LiDAR point cloud generated with a "Phenomobile". *Front. Plant Sci.* **2019**, *10*, 554. [CrossRef] [PubMed]
115. Park, E.S.; Kumar, A.P.; Arief, M.A.A.; Joshi, R.; Lee, H.; Cho, B.K. Noncontact measurements of the morphological phenotypes of sorghum using 3D LiDAR point cloud. *Korean J. Agric. Sci.* **2022**, *49*, 483–493. [CrossRef]
116. Shi, Y.; Wang, N.; Taylor, R.K.; Raun, W.R. Improvement of a ground-LiDAR-based corn plant population and spacing measurement system. *Comput. Electron. Agric.* **2015**, *112*, 92–101. [CrossRef]
117. Hyyppa, J.; Hyyppa, H.; Leckie, D.; Gougeon, F.; Yu, X.; Maltamo, M. Review of methods of small-footprint airborne laser scanning for extracting forest inventory data in boreal forests. *Int. J. Remote Sens.* **2008**, *29*, 1339–1366. [CrossRef]
118. Lucas, R.M.; Lee, A.C.; Bunting, P.J. Retrieving forest biomass through integration of CASI and LiDAR data. *Int. J. Remote Sens.* **2008**, *29*, 1553–1577. [CrossRef]
119. Eitel, J.U.; Vierling, L.A.; Magney, T.S. A lightweight, low-cost autonomously operating terrestrial laser scanner for quantifying and monitoring ecosystem structural dynamics. *Agric. For. Meteorol.* **2013**, *180*, 86–96. [CrossRef]
120. Kankare, V.; Holopainen, M.; Vastaranta, M.; Puttonen, E.; Yu, X.; Hyyppä, J.; Vaaja, M.; Hyyppä, H.; Alho, P. Individual tree biomass estimation using terrestrial laser scanning. *ISPRS J. Photogramm. Remote Sens.* **2013**, *75*, 64–75. [CrossRef]
121. Saeys, W.; Lenaerts, B.; Craessaerts, G.; De Baerdemaeker, J. Estimation of the crop density of small grains using LiDAR sensors. *Biosyst. Eng.* **2009**, *102*, 22–30. [CrossRef]
122. Rosli, S.; Hashim, F.; Raj, T.; Zaki, W.M.D.W.; Hussain, A. A rapid technique in evaluating tree health using LiDAR sensors. *Int. J. Eng. Technol.* **2018**, *7*, 118–122. [CrossRef]
123. Thi Phan, A.T.; Takahashi, K.; Rikimaru, A.; Higuchi, Y. Method for estimating rice plant height without ground surface detection using laser scanner measurement. *J. Appl. Remote Sens.* **2016**, *10*, 046018. [CrossRef]
124. Sun, S.; Li, C.; Paterson, A.H. In-field high-throughput phenotyping of cotton plant height using LiDAR. *Remote Sens.* **2017**, *9*, 377. [CrossRef]
125. Blanquart, J.E.; Sirignano, E.; Lenaerts, B.; Saeys, W. Online crop height and density estimation in grain fields using LiDAR. *Biosyst. Eng.* **2020**, *198*, 1–14. [CrossRef]
126. Madec, S.; Baret, F.; de Solan, B.; Thomas, S.; Dutartre, D.; Jezequel, S.; Hemmerlé, M.; Colombeau, G.; Comar, A. High-throughput phenotyping of plant height: Comparing unmanned aerial vehicles and ground LiDAR estimates. *Front. Plant Sci.* **2017**, *8*, 2002. [CrossRef]
127. Harkel, J.; Bartholomeus, H.; Kooistra, L. Biomass and crop height estimation of different crops using UAV-based LiDAR. *Remote Sens.* **2019**, *12*, 17. [CrossRef]
128. Tilly, N.; Hoffmeister, D.; Liang, H.; Cao, Q.; Liu, Y.; Lenz-Wiedemann, V.; Miao, Y.; Bareth, G. Evaluation of terrestrial laser scanning for rice growth monitoring. *Int. Arch. Photogramm. Remote Sens. Spat. Inf. Sci.* **2012**, *39*, 351–356. [CrossRef]
129. Xiao, S.; Chai, H.; Shao, K.; Shen, M.; Wang, Q.; Wang, R.; Sui, Y.; Ma, Y. Image-based dynamic quantification of aboveground structure of sugar beet in field. *Remote Sens.* **2020**, *12*, 269. [CrossRef]
130. Greaves, H.E.; Vierling, L.A.; Eitel, J.U.; Boelman, N.T.; Magney, T.S.; Prager, C.M.; Griffin, K.L. Estimating aboveground biomass and leaf area of low-stature Arctic shrubs with terrestrial LiDAR. *Remote Sens. Environ.* **2015**, *164*, 26–35. [CrossRef]
131. Chen, Y.; Zhu, H.; Ozkan, H.E. Development of a variable-rate sprayer with laser scanning sensor to synchronize spray outputs to tree structures. *Trans. ASABE* **2012**, *55*, 773–781. [CrossRef]
132. Hu, M.; Whitty, M. An evaluation of an apple canopy density mapping system for a variable-rate sprayer. *IFAC-PapersOnLine* **2019**, *52*, 342–348. [CrossRef]
133. Jeon, H.Y.; Zhu, H. Development of a variable-rate sprayer for nursery liner applications. *Trans. ASABE* **2012**, *55*, 303–312. [CrossRef]
134. Llorens, J.; Gil, E.; Llop, J.; Escolà, A. Variable rate dosing in precision viticulture: Use of electronic devices to improve application efficiency. *Crop Protect.* **2010**, *29*, 239–248. [CrossRef]
135. Shen, Y.; Addis, D.; Liu, H.; Hussain, F. A LIDAR-Based Tree Canopy Characterization under Simulated Uneven Road Condition: Advance in Tree Orchard Canopy Profile Measurement. *J. Sens.* **2017**, *2017*, 8367979. [CrossRef]
136. Tilly, N.; Aasen, H.; Bareth, G. Fusion of plant height and vegetation indices for the estimation of barley biomass. *Remote Sens.* **2015**, *7*, 11449–11480. [CrossRef]
137. Berk, P.; Stajnko, D.; Belsak, A.; Hocevar, M. Digital evaluation of leaf area of an individual tree canopy in the apple orchard using the LiDAR measurement system. *Comput. Electron. Agric.* **2020**, *169*, 105158. [CrossRef]
138. Chakraborty, M.; Khot, L.R.; Sankaran, S.; Jacoby, P.W. Evaluation of mobile 3D light detection and ranging based canopy mapping system for tree fruit crops. *Comput. Electron. Agric.* **2019**, *158*, 284–293. [CrossRef]
139. Mahmud, M.S.; Zahid, A.; He, L.; Choi, D.; Krawczyk, G.; Zhu, H.; Heinemann, P. Development of a LiDAR-guided section-based tree canopy density measurement system for precision spray applications. *Comput. Electron. Agric.* **2021**, *182*, 106053. [CrossRef]
140. Pforte, F.; Selbeck, J.; Hensel, O. Comparison of two different measurement techniques for automated determination of plum tree canopy cover. *Biosyst. Eng.* **2012**, *113*, 325–333. [CrossRef]

141. Hosoi, F.; Omasa, K. Voxel-based 3-D modeling of individual trees for estimating leaf area density using high-resolution portable scanning LiDAR. *IEEE Trans. Geosci. Remote Sens.* **2006**, *44*, 3610–3618. [CrossRef]
142. Rinaldi, M.; Llorens, J.; Gil, E. Electronic characterization of the phenological stages of grapevine using a LIDAR sensor. In *Precision Agriculture*; Wageningen Academic: Gelderland, The Netherlands, 2013; pp. 601–609.
143. Llorens, J.; Gil, E.; Llop, J.; Queraltó, M. Georeferenced LiDAR 3D vine plantation map generation. *Sensors* **2011**, *11*, 6237–6256. [CrossRef] [PubMed]
144. Newnham, G.; Goodwin, N.; Armston, J.; Muir, J.; Culvenor, D. Comparing time-of-flight and phase-shift terrestrial laser scanners for characterising topography and vegetation density in a forest environment. In Proceedings of the SilviLaser, Vancouver, BC, Canada, 16–19 September 2012.
145. Rosell, J.R.; Llorens, J.; Sanz, R.; Arnó, J.; Ribes-Dasi, M.; Masip, J.; Escolà, A.; Camp, F.; Solanelles, F.; Gràcia, F.; et al. Obtaining the three-dimensional structure of tree orchards from remote 2D terrestrial LIDAR scanning. *Agric. For. Meteorol.* **2009**, *149*, 1505–1515. [CrossRef]
146. Garrido, M.; Paraforos, D.S.; Reiser, D.; Vázquez Arellano, M.; Griepentrog, H.W.; Valero, C. 3D maize plant reconstruction based on georeferenced overlapping LiDAR point clouds. *Remote Sens.* **2015**, *7*, 17077–17096. [CrossRef]
147. Underwood, J.P.; Hung, C.; Whelan, B.; Sukkarieh, S. Mapping almond orchard canopy volume, flowers, fruit and yield using lidar and vision sensors. *Comput. Electron. Agric.* **2016**, *130*, 83–96. [CrossRef]
148. Garrido, M.; Méndez, V.; Valero, C.; Correa, C.; Torre, A.; Barreiro, P. Online dose optimization applied on tree volume through a laser device. In Proceedings of the First International Conference on Robotics and Associated High-technologies and Equipment for Agriculture, Pisa, Italy, 19–21 September 2012; pp. 325–330.
149. Lee, S.; Lee, D.; Choi, P.; Park, D. Accuracy–power controllable LiDAR sensor system with 3D object recognition for autonomous vehicle. *Sensors* **2020**, *20*, 5706. [CrossRef] [PubMed]
150. Béland, M.; Baldocchi, D.D.; Widlowski, J.L.; Fournier, R.A.; Verstraete, M.M. On seeing the wood from the leaves and the role of voxel size in determining leaf area distribution of forests with terrestrial LiDAR. *Agric. For. Meteorol.* **2014**, *184*, 82–97. [CrossRef]
151. Xianping, G.; Kuan, L.; Baijing, Q.; Xiaoya, D.; Xinyu, X. Extraction of geometric parameters of soybean canopy by airborne 3D laser. *Trans. Chin. Soc. Agric. Eng.* **2019**, *35*, 96–103.
152. Zhang, M.; Ji, Y.; Li, S.; Cao, R.; Xu, H.; Zhang, Z. Research progress of agricultural machinery navigation technology. *Nongye Jixie Xuebao/Trans. Chin. Soc. Agric. Mach.* **2020**, *51*.
153. Reger, M.; Stumpenhausen, J.; Bernhardt, H. Evaluation of LiDAR for the free navigation in agriculture. *AgriEngineering* **2022**, *4*, 489–506. [CrossRef]
154. Jiang, A.; Ahamed, T. Navigation of an Autonomous Spraying Robot for Orchard Operations Using LiDAR for Tree Trunk Detection. *Sensors* **2023**, *23*, 4808. [CrossRef]
155. Garrido-Izard, M.; Pérez-Ruiz, M.; Valero, C.; Gliever, C.J.; Hanson, B.D.; Slaughter, D.C. Active optical sensors for tree stem detection and classification in nurseries. *Sensors* **2014**, *14*, 10783–10803. [CrossRef] [PubMed]
156. Xie, D.; Xu, Y.; Wang, R. Obstacle detection and tracking method for autonomous vehicle based on three-dimensional LiDAR. *Int. J. Adv. Robot. Syst.* **2019**, *16*, 1729881419831587. [CrossRef]
157. Nuchter, A.; Lingemann, K.; Hertzberg, J.; Surmann, H. 6D SLAM with approximate data association. In Proceedings of the 12th International Conference on Advanced Robotics, IEEE, Seattle, WA, USA, 18–20 July 2005; pp. 242–249.
158. Sack, D.; Burgard, W. A comparison of methods for line extraction from range data. *IFAC Proc. Vol.* **2004**, *37*, 728–733. [CrossRef]
159. Oliveira, M.; Santos, V.; Sappa, A.; Dias, P. Scene representations for autonomous driving: An approach based on polygonal primitives. In *Second Iberian Robotics Conference, Volume 1*; Springer: Berlin/Heidelberg, Germany, 2015; pp. 503–515.
160. Matei, B.C.; Vander Valk, N.; Zhu, Z.; Cheng, H.; Sawhney, H.S. Image to lidar matching for geotagging in urban environments. In Proceedings of the IEEE Workshop on Applications of Computer Vision (WACV), Clearwater Beach, FL, USA, 17–18 January 2013; pp. 413–420.
161. Wu, Y.; Wang, Y.; Zhang, S.; Ogai, H. Deep 3D object detection networks using LiDAR data: A review. *IEEE Sens. J.* **2020**, *21*, 1152–1171. [CrossRef]
162. Sharma, M.; Garg, R.D.; Badenko, V.; Fedotov, A.; Min, L.; Yao, A. Potential of airborne LiDAR data for terrain parameters extraction. *Quat. Int.* **2021**, *575*, 317–327. [CrossRef]
163. Jaspers, H.; Himmelsbach, M.; Wuensche, H.J. Multi-modal local terrain maps from vision and lidar. In Proceedings of the Intelligent Vehicles Symposium (IV), Redondo Beach, CA, USA, 11–14 June 2017; pp. 1119–1125.
164. De Agirre, A.M.; Malpica, J.A. Constructing a digital terrain model from LiDAR data. *Adv. Geoinf. Technol.* **2010**, 47–59.
165. Bayram, E.; Frossard, P.; Vural, E.; Alatan, A. Analysis of airborne LiDAR point clouds with spectral graph filtering. *IEEE Geosci. Remote Sens. Lett.* **2018**, *15*, 1284–1288. [CrossRef]
166. Lin, H.; Ai, C.; Xu, Q.; Sun, X.; Zhao, H. Lidar based vineyard path identification approach to plant protection robot autonomous driving. In Proceedings of the IEEE International Conference on Real-time Computing and Robotics (RCAR), Irkutsk, Russia, 4–9 August 2019; pp. 516–520.
167. Wang, P.; Gu, T.; Sun, B.; Huang, D.; Sun, K. Research on 3D point cloud data preprocessing and clustering algorithm of obstacles for intelligent vehicle. *World Electr. Veh. J.* **2022**, *13*, 130. [CrossRef]

168. Iwasaki, K.; Shimoda, S.; Nakata, Y.; Hayamizu, M.; Nanko, K.; Torita, H. Remote sensing of soil ridge height to visualize windbreak effectiveness in wind erosion control: A strategy for sustainable agriculture. *Comput. Electron. Agric.* **2024**, *219*, 108778. [CrossRef]
169. Kuras, A.; Brell, M.; Rizzi, J.; Burud, I. Hyperspectral and lidar data applied to the urban land cover machine learning and neural-network-based classification: A review. *Remote Sens.* **2021**, *13*, 3393. [CrossRef]
170. Sun, P.; Zhao, X.; Xu, Z.; Wang, R.; Min, H. A 3D LiDAR data-based dedicated road boundary detection algorithm for autonomous vehicles. *IEEE Access* **2019**, *7*, 29623–29638. [CrossRef]
171. Gharineiat, Z.; Tarsha Kurdi, F.; Campbell, G. Review of automatic processing of topography and surface feature identification LiDAR data using machine learning techniques. *Remote Sens.* **2022**, *14*, 4685. [CrossRef]
172. Qin, J.; Sun, R.; Zhou, K.; Xu, Y.; Lin, B.; Yang, L.; Wu, C. Lidar-based 3D obstacle detection using focal voxel R-CNN for farmland environment. *Agronomy* **2023**, *13*, 650. [CrossRef]
173. Doerr, Z.; Mohsenimanesh, A.; Laguë, C.; McLaughlin, N.B. Application of the LIDAR technology for obstacle detection during the operation of agricultural vehicles. *Can. Biosyst. Eng. J.* **2013**, *55*. [CrossRef]
174. Periu, C.F.; Mohsenimanesh, A.; Laguë, C.; McLaughlin, N.B. Isolation of vibrations transmitted to a LIDAR sensor mounted on an agricultural vehicle to improve obstacle detection. *Can. Biosyst. Eng. J.* **2013**, *55*. [CrossRef]
175. Reina, G.; Milella, A.; Rouveure, R.; Nielsen, M.; Worst, R.; Blas, M.R. Ambient awareness for agricultural robotic vehicles. *Biosyst. Eng.* **2016**, *146*, 114–132. [CrossRef]
176. Yuhan, J.; Shichao, L.; Cheng, P.; Hongzhen, X.; Ruyue, C.; Man, Z. Obstacle detection and recognition in farmland based on fusion point cloud data. *Comput. Electron. Agric.* **2021**, *189*, 106409.
177. Farm Equipment Accidents. Farm Equipment Accidents (Online Images). 2014. Available online: http://www.redpowermagazine.com/forums/topic/59807-farm-equipment-accidents/ (accessed on 3 December 2023).
178. Rovira-Más, F.; Saiz-Rubio, V.; Cuenca-Cuenca, A. Augmented perception for agricultural robots navigation. *IEEE Sens. J.* **2020**, *21*, 11712–11727. [CrossRef]
179. Bai, Z.; Bi, D.; Wu, J.; Wang, M.; Zheng, Q.; Chen, L. Intelligent driving vehicle object detection based on improved AVOD algorithm for the fusion of LiDAR and visual information. *Actuators* **2022**, *11*, 272. [CrossRef]
180. Yang, T.; Bai, Z.; Li, Z.; Feng, N.; Chen, L. Intelligent vehicle lateral control method based on feedforward+ predictive LQR algorithm. *Actuators* **2021**, *10*, 228. [CrossRef]
181. Wang, G.; Wu, J.; He, R.; Yang, S. A point cloud-based robust road curb detection and tracking method. *IEEE Access* **2019**, *7*, 24611–24625. [CrossRef]
182. Yehua, S.; Guangqiang, Z.; Zhijun, M.; Hao, W.; Chunhua, S.; Zhenghe, S. Field obstacle detection method of 3D Lidar point cloud based on Euclidean clustering. *Nongye Jixie Xuebao/Trans. Chinese Soc. Agric. Mach.* **2022**, *53*.
183. Gao, F.; Li, C.; Zhang, B. A dynamic clustering algorithm for LiDAR obstacle detection of autonomous driving system. *IEEE Sens. J.* **2021**, *21*, 25922–25930. [CrossRef]
184. Qi, C.R.; Su, H.; Mo, K.; Guibas, L.J. PointNet: Deep learning on point sets for 3D classification and segmentation. In Proceedings of the IEEE Conference on Computer Vision and Pattern Recognition, Honolulu, HI, USA, 21–26 July 2017; pp. 652–660.
185. Li, J.; Zhang, Y.; Liu, X.; Zhang, X.; Bai, R. Obstacle detection and tracking algorithm based on multi-lidar fusion in urban environment. *IET Intell. Transp. Syst.* **2021**, *15*, 1372–1387. [CrossRef]
186. Muresan, M.P.; Nedevschi, S. Multimodal sparse LIDAR object tracking in clutter. In Proceedings of the IEEE 14th International Conference on Intelligent Computer Communication and Processing (ICCP), Cluj-Napoca, Romania, 6–8 September 2018; pp. 215–221.
187. Lang, A.H.; Vora, S.; Caesar, H.; Zhou, L.; Yang, J.; Beijbom, O. PointPillars: Fast encoders for object detection from point clouds. In Proceedings of the IEEE/CVF Conference on Computer Vision and Pattern Recognition, Long Beach, CA, USA, 15–20 June 2019; pp. 12697–12705.
188. Wu, W.; Qi, Z.; Fuxin, L. PointConv: Deep convolutional networks on 3D point clouds. In Proceedings of the IEEE/CVF Conference on Computer Vision and Pattern Recognition, Long Beach, CA, USA, 15–20 June 2019; pp. 9621–9630.
189. Cheng, J.; Xiang, Z.; Cao, T.; Liu, J. Robust vehicle detection using 3D LiDAR under complex urban environment. In Proceedings of the IEEE International Conference on Robotics and Automation (ICRA), Hong Kong, China, 31 May–5 June 2014; pp. 691–696.
190. Kim, T.; Park, T.H. Extended Kalman filter (EKF) design for vehicle position tracking using reliability function of radar and LiDAR. *Sensors* **2020**, *20*, 4126. [CrossRef]
191. del Pino, I.; Vaquero, V.; Masini, B.; Sola, J.; Moreno-Noguer, F.; Sanfeliu, A.; Andrade-Cetto, J. Low resolution lidar-based multi-object tracking for driving applications. In *Third Iberian Robotics Conference*; Springer: Berlin/Heidelberg, Germany, 2017; pp. 287–298.
192. Shang, Y.; Wang, H.; Qin, W.; Wang, Q.; Liu, H.; Yin, Y.; Meng, Z. Design and test of obstacle detection and harvester pre-collision system based on 2D lidar. *Agronomy* **2023**, *13*, 388. [CrossRef]
193. Hamano, M.; Shiozawa, S.; Yamamoto, S.; Suzuki, N.; Kitaki, Y.; Watanabe, O. Development of a method for detecting the planting and ridge areas in paddy fields using AI, GIS, and precise DEM. *Precis. Agric.* **2023**, *24*, 1862–1888. [CrossRef]
194. Luna-Santamaria, J.; Martínez de Dios, J.R.; Ollero Baturone, A. LIDAR-based detection of furrows for agricultural robot autonomous navigation. In *XLIII Jornadas de Automática*; Universidade da Coruña—Servizo de Publicacións: A Coruña, Spain, 2022; pp. 728–734.

195. Ren, S.; He, K.; Girshick, R.; Sun, J. Faster R-CNN: Towards real-time object detection with region proposal networks. *IEEE Trans. Pattern Anal. Mach. Intell.* **2016**, *39*, 1137–1149. [CrossRef]
196. Behroozpour, B.; Sandborn, P.A.; Wu, M.C.; Boser, B.E. LiDAR system architectures and circuits. *IEEE Commun. Mag.* **2017**, *55*, 135–142. [CrossRef]
197. Gomes, T.; Roriz, R.; Cunha, L.; Ganal, A.; Soares, N.; Araújo, T.; Monteiro, J. Evaluation and testing system for automotive LiDAR sensors. *Appl. Sci.* **2022**, *12*, 13003. [CrossRef]
198. Zlocki, A.; Klas, C.; Schulte, K.; Kradepohl, U. Definition and application of a test methodology for lidar sensors. *ATZelectronics Worldw.* **2021**, *16*, 46–49. [CrossRef]
199. Park, J.; Cho, J.; Lee, S.; Bak, S.; Kim, Y. An automotive LiDAR performance test method in dynamic driving conditions. *Sensors* **2023**, *23*, 3892. [CrossRef] [PubMed]
200. NHTSA. *LIDAR Speed-Measuring Device Performance Specifications*; Report No. DOT HS 809 81; National Highway Traffic Safety Administration: Washington, DC, USA, 2013.
201. Aspiras, T.H.; Asari, V.K.; Bradley, C.; Gnacek, A.; Kershner, C.; LeMaster, D.A.; McManamon, P.F.; Reinhardt, A.D.; Ruff, E.; Valenta, C.R.; et al. Toward standardized testing of automotive lidars: Year two results. *Opt. Eng.* **2024**, *63*, 085102. [CrossRef]
202. Heidemann, H.K. *Lidar Base Specification Techniques and Methods, ver. 1.3*; U.S. Geological Survey: Reston, VA, USA, 2018; Volume 11, Chapter B4; p. 101. [CrossRef]
203. Beiker, S. *Next-Generation Sensors for Automated Road Vehicles*; Report EPR2023003; SAE Research: Warrendale, PA, USA, 2023. [CrossRef]
204. Rachakonda, P.; Mane, A.; Schlenoff, C.; Saidi, K. Methods to evaluate 3D lidars used for automated driving. *Measurement* **2025**, *239*, 115464. [CrossRef]
205. Elster, L.; Staab, J.P.; Peters, S. Making Automotive Radar Sensor Validation Measurements Comparable. *Appl. Sci.* **2023**, *13*, 11405. [CrossRef]
206. Fan, Y.C.; Zheng, L.J.; Liu, Y.C. 3D environment measurement and reconstruction based on LiDAR. In Proceedings of the 2018 IEEE International Instrumentation and Measurement Technology Conference (I2MTC), Houston, TX, USA, 14–17 May 2018; pp. 1–4.
207. dos Santos, J.B. Proof-of-Concept of a Single-Point Time-of-Flight LiDAR System and Guidelines Towards Integrated High-Accuracy Timing, Advanced Polarization Sensing and Scanning with a MEMS Micromirror. Master's Thesis, Universidade do Minho, Braga, Portugal, 2018.
208. WHY HESAI LEADS ISO/PWI 13228 Test Method Standard for Lidar. July 2022. AEM. Available online: https://www.autoelectronics.co.kr/article/articleView.asp?idx=4763 (accessed on 4 December 2024).
209. Hokuyo Automatic Co., Ltd. UTM-30LX: Scanning Laser Range Finder. Hokuyo Automatic. (n.d.). Available online: https://www.hokuyo-aut.jp/products/data.php?id=112 (accessed on 12 October 2024).
210. Hokuyo Automatic Co., Ltd. The Standards for Safety LiDAR. Available online: https://www.hokuyo-aut.jp/products/data.php?id=112 (accessed on 12 October 2024).
211. Boehler, W.; Vicent, M.B.; Marbs, A. Investigating laser scanner accuracy. *Int. Arch. Photogramm. Remote Sens. Spat. Inf. Sci.* **2003**, *34*, 696–701.